Additive Manufacturing Process Investigation for the Fabrication of Composite Scaffolds for Soft Tissue Application

by

PARIMAL THAKORBHAI PATEL

Presented to the Faculty of the Graduate School of
The University of Texas at Arlington in Partial Fulfillment
of the Requirements
for the Degree of

Master of Science

THE UNIVERSITY OF TEXAS AT ARLINGTON
May 2018

Acknowledgments

I would like to thank my supervising professor Dr. Panos Shiakolas for giving me an opportunity to work in MARS lab. I am grateful to Dr. Tre Welch for providing material for conducting research and providing valuable inputs throughout the research work. I would like to thank Dr. Pranesh Aswath for being on my thesis committee and providing valuable inputs. I am thankful to Mechanical and Aerospace Engineering Department at the University of Texas at Arlington for providing facilities and resources. Also, I would like to thank my colleagues Dr. Prashath Ravi, Dr. to be Chris Abrego, Tushar Saini, Kashish Dhal, Ravi Patel, Sudip Hazra, and Jon Daniel for their guidance and help.

Abstract

Additive Manufacturing Process Investigation for the Fabrication of Composite Scaffolds for Soft Tissue Application

Parimal Thakorbhai Patel, MS

The University of Texas at Arlington, 2018

Supervising Professor: Panos S. Shiakolas

Additive manufacturing has been investigated and employed in the bio-medical domain for the fabrication of various devices and scaffolds. In various soft tissue engineering applications, multi-functional multi-material scaffolds are required for cell proliferation, structural integrity, bio-compatibility and tissue regeneration. In this research, an additive manufacturing methodology is developed to allow the fabrication of bio-composite scaffolds using a multi-modality in-house built platform. The researched materials for printing are Poly-L-Lactic Acid (PLLA) and a newly developed photo-curable radiopaque polymer called Rylar (Poly glycerole sebacate fumarate gadodiamide) mixed with a cross-linking agent Poly (Ethylene glycol) diacrylate (PEGDA). The developed methodology uses a Fused Filament Fabrication (FFF) technique to print PLLA and Direct Ink Writing (DIW) or Viscous Extrusion (VE) to process Rylar in-situ on the same platform. Controlled process parameters of print speed, feed speed, UV intensity, and nozzle to bed distance were investigated to fabricate scaffolds. Multi-layered composite scaffolds with two materials

were successfully printed. Further investigation is proposed towards the fabrication of bio-scaffolds with more layers of each material for soft tissue application such as tracheomalacia.

LIST OF ILLUSTRATIONS

LIST OF TABLES

TABLE OF CONTENTS

CHAPTER 1

Introduction

1.1 Background of Additive Manufacturing

Additive manufacturing (AM) dates back to 1980, when Hideo Kodama from Nagoya Municipal Industrial Research Institute developed a device in 1981 which used Ultraviolet (UV) to cure photo-reactive polymer. In 1984, Chuck Hall invented Stereolithography and filed a patent for the process [2]. In the process, the object was created by adding a layer on top of another layer while curing photo polymers using UV. Hull defined the process as a "system for generating three-dimensional objects by creating a cross-sectional pattern of the object to be formed" [3] [4]. Meanwhile in 1988, Carl Deckard filed a patent for another additive manufacturing technique, Selective Laser Sintering (SLS) [5]. Laser sintering technique has become one of the most used processes for creating end user parts of metals in todays world. While Hall founded 3D Systems Corporation, Scott Crump came up with the new methodology of Fused Deposition Modeling (FDM) which is a streamline technology today and established Stratasys. In FDM or Fused Filament Fabrication (FFF), thermo-plastic materials in form of filament are used to build a part layer by layer. Within the span of ten years, three main processes defined the new era and the additive manufacturing became prominent methodology for Rapid Prototyping. It has acquired new name of 3D printing when the researchers and hobbyist started to explore this field.

While 3D Systems and Stratasys were commercializing their respective technologies, many more companies like EOS GmBH, Electro Optical Systems (EOS), Cubital, Helisys started to explore possibilities with their own stereolithography and

FDM machines [6]. A major history defining moment came when RepRap project was initiated in 2005 [7]. The open source project, Replicated Rapid Prototyper (RepRap), aimed at making affordable 3D printer which could replicate itself easily. Started by Adrian Bowyer, a senior lecturer at the University of Bath, the project attracted many collaborators. In the previous decade, FDM has become more accessible than any other additive manufacturing processes due to collaboration in public domain and drop in desktop printer prices.

Additive manufacturing is finding major applications in industries, bio-medical field, and prototyping of user designs. AM techniques like Laser Beam Melting (LBM), Selective Laser Sintering (SLS), and Electron beam melting (EBM) have been widely used by manufactures to process materials like steel, titanium, and aluminum alloys [8]. SLM Solutions (Lubeck, Germany) has developed selective laser melting machines to process metal powders of titanium, cobalt-chrome, and nickel based alloys [9]. Development in medical applications came when 3D printing was used to fabricate scaffolds for tissue engineered bladders and prosthetic limbs [10] [11]. A scaffold is a template or a support structure which is used for tissue regeneration. Though innovation has begun, the world will have to wait many years to see accelerated growth in organ transplants using additive manufacturing. 3D printing technique was used currently by OpenBionics (Bristol, United Kingdom) to make a prosthetic arm (https://openbionics.com/hero-arm/). Tarek and his team have developed an open source template to 3D print a stethoscope from ABS (Acrylonitrile butadiene styrene) plastic at very low cost which can be used in developing countries or war zone areas where medical supply is not easily available [12]. Another impact of AM is on scaffolding for tissue engineering applications. The ability to 3D print customize scaffolds has lead to treatment of individual case for tissue regeneration [13]. Also, different biocompatible materials address the issue of foreign material coming

in contact with human cells and organs [14] [15]. CellInk (Gothenburg, Sweden) has developed bio-ink for regenerative tissue applications (https://cellink.com/bioink/). Mikoajewska et al. [16], Peltola et al. [17], and Yeong et al. [18] have discussed 3D printing techniques such as multi-nozzle deposition manufacturing, Robocasting, and Pressure-assisted micro-syringe for tissue engineering applications.

1.2 Literature Review

The scaffold structure plays a major role in tissue engineering applications. Cell and tissue proliferation highly depend on fiber size, pore size, and porosity [19]. Conventional techniques to fabricate micro-porous and nano-fibrous scaffolds include solvents based scaffolds, electrospining, freeze-drying, phase separation, and self assembly [20]. For bone tissue engineering application, materials like hydroxy appetite, Beta-TCP (tricalcium phosphate) ceramics [21], and bio-active glasses have been used to manufacture scaffolds [22]. Bio-degradable materials from polymers, magnesium alloys, and ceramics have made great progress [23]. In area of soft tissue engineering applications, materials like Poly-L-lactic acid (PLLA) and Poly (glycerol sebacate) have been explored by Xuejun et al. and Yi-Cheun et al. respectively [23] [24]. Bio-degradable polymer materials have been widely used for regenerative tissue engineering. With inter connected macroporous and nanofibrous structure, matrix created by PLLA can be an excellent structure for cell proliferation [19].

On the other hand, conventional techniques for fabrication of scaffolds have certain limitations in terms of process characterization, repeatability, and under defined variability in terms of structure. Additive manufacturing techniques open up a great opportunity to fabricate tailored and in-situ manufacturing of scaffolds [25]. Different techniques of 3D printing like Fused Filament Fabrication (FFF), Stereolithogrpahy (SLA), Inkjet (IJ), Electrohydrodynamic printing, Pneumatic based extrusion, and

Direct Ink writing (DIW) have been explored by researchers and companies to address the limitations of 3D printing in biomedical field [26] [27]. Human organs and bones require heterogeneous structure for cell proliferation and in-vivo tissue generation. Current technologies are restricted to process single material [28]. A multi-process technique can facilitate manufacturing of multi-material scaffolds to address the issue of heterogeneous structure required for human body.

In this research, a process to combine two different methodologies, FFF and DIW, to fabricate composite scaffolds was explored. Bio-degradable materials, PLLA and newly developed Poly Glycerol Sebacate Fumarate Gadodiamide (Rylar) mixed with cross-linking agent Poly Ethylene Glycerol Diacrylate (PEGDA) were used. Such scaffolds can be used in the treatment of tracheomalacia. Feasibility of novel polymer, Rylar, for medical applications has been explored by Goodfriend et al. [29]. Research by Ravi et al. suggests the possibility of processing Rylar using DIW technique to print scaffolds with Young's modulus (E) closely matching with human cartilages and storage moduli (E') with bovine cartilages [30].

1.3 Trachea and Tracheomalacia

Human trachea is a windpipe or an airway in throat that carries air in and out of the body. Human trachea is made of fifteen to twenty semi-annular rings of cartilages as represented in figure 1.1a [1]. It lengthens and dilates during inspiration while during expiration it narrows and shortens. Tracheomalacia is the collapse of the trachea due to softness of cartilages as represented in figure 1.1b [1]. It causes the airway to narrow during exhalation leading to breathing problem.

"Tracheomalacia can be categorized into three groups on the basis of histologic, endoscopic, and clinical presentation, as follow

- Type I: Congenital or intrinsic tracheal abnormalities that can be associated with a tracheoesophageal fistula or esophageal atresia.
- Type II: Extrinsic defects or anomalies, such as a vascular ring causing undue pressure on the trachea.
- Type III: Acquired tracheomalacia that occurs with prolonged intubation, chronic tracheal infections, or inflammatory conditions like relapsing polychondritis" [31].

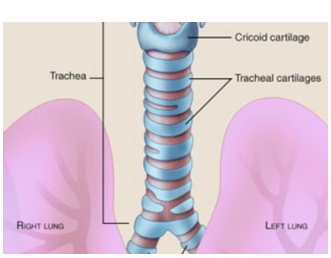

(a) Human Trachea

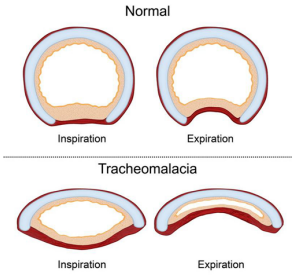

(b) orva-tracheomalacia

Figure 1.1: Normal and abnormal trachea [1]

Congenital tracheomalacia is usually seen between 4 to 8 weeks of age in infants. Some have mild forms while the condition for others can be severe and require immediate attention. No definite numbers are available for the cases of tracheomalacia in infants but it occurs in approximately 1 in 2100 children [32]. Tracheomalacia was diagnosed in 160 children (94 males) at a median age of 4.0 years (range, 0-17 years) at Sophia Children's Hospital, Netherlands [31] [33]. Altman identified 42 cases of pediatric airway tracheomalacia over a 5-year period and Burden et al. recorded 62 cases in Pediatric Intensive Care (Royal Children's Hospital, Parkville, Australia) in the period 1986 to 1995, although they believe that the condition is under-diagnosed

[34]. Greenholz and Karrer treated 41 infants for tracheomalacia during 7 years at the Department of Surgery, University of Colorado, Denver [35].

Diagnosis usually starts with a physical exam and the patients medical history. Bronchoscopy is performed to view the airway (windpipe) to diagnose tracheomalacia. Additional tests like CT (Computed Tomography) scan, dynamic MRI (Magnetic Resonance Imaging), and fluoroscopy are also performed. Sometimes tracheomalacia is incorrectly diagnosed as asthma. It is important that a child's doctor has lot of experience in diagnosing and treatments. Tracheomalacia is often self-limited and resolves itself by the second year of life. But severe case requires treatments which include pharmacotherapy, positive pressure, and surgery. The treatments are characterized for each individual depending on type and location of tracheomalacia. "Following are the surgical options.

- Aortopexy: This surgery opens up the trachea by moving up the aorta (the bodys main blood vessel) and attaching it to the back of the breastbone (sternum).
- Tracheopexy: Similar to an aortopexy, this procedure opens up and supports the airway by suspending the front of the tracheal wall from the back of the sternum. Sometimes the thymus gland is removed to create more space between the aorta and the sternum
- Placing a stent: A metal stent is inserted orally and expanded in trachea to keep it open" [36].

Surgical options have complex operations as they include suturing. Also, individual case requires different treatments. Inserting a metal stent can lead to granulation tissue formation because of the external metal coming in contact with cells. It has low but significant failure rate and it does not have universal success rate [37].

Here, a new treatment is proposed where a bio-degradable and bio-resorbbale tube can be placed inside trachea. The tube will work as a scaffold in which tissue regeneration can occur through cell proliferation. Use of bio-resorbable material can address the issue of granulation tissue formation. Also, bio-degradable material can help to avoid extra surgical operation after the trachea has developed fully. On the other hand, AM allows to fabricate scaffolds with tailored properties which can be useful in the treatment of individual case of tracheomalacia. Proposed research is aimed at one of the life-threatening defects of Tracheomalacia in children.

1.4 Scope of the research and outline of the thesis

A close observation of human trachea reveals that cartilages are connected through muscles. To fabricate a similar structure, two different materials can be used where one can serve the purpose of stiff cartilages and another can be flexible as muscles. Here, PLLA can be used as a stiff material while the novel polymer, Rylar, which has visco-elastic behavior post curing can be used as flexible material. Proposed research includes integration of two AM techniques, FFF and DIW, to process PLLA and Rylar respectively. Understanding of each implemented AM process is required. Preliminary experiments were carried out with FFF technique to process PLLA and understand the effects of process parameters such as print speed (S), nozzle to bed distance (NBD), and bed surface. For processing Rylar using DIW, process parameters such as UV intensity, print speed, in-fill density, and infill pattern were considered. A unique combination of FFF and DIW techniques was used and a methodology was investigated to fabricate biodegradable composite scaffolds. Bonding between the two materials was investigated since used materials were never combined before. Also, limitations of open-source software Silc3r with respect to multi-material printing were addressed through this research. The developed methodology was implemented

on an in-house multi-modality 3D printer to print composite scaffolds and challenges faced during the experiments were addressed. In the end, multi layered structure with Rylar being sandwiched between PLLA was 3D printed in a single run to evaluate possibility of fabricating multi-layered structure with recommended materials. The aim of this research is to develop an AM methodology to combine two different materials in a single process and fabricate composite scaffolds which can have a prospective application in soft tissue engineering.

Outline of the thesis is as follow:

- Chapter 1: The background of additive manufacturing with current developments is discussed in the introduction section. A literature review related to applications of additive manufacturing in bio-medical field is included. Finally, the scope of research is summarized with thesis outline.
- Chapter 2: In this chapter, used multi-modality 3D printer for research is described to understand the process parameters of AM. FFF and DIW modules are discussed in details with a quick overview of their possible combination on an existing multi-modality platform.
- Chapter 3: This chapter includes details of the investigation to develop a methodology for combining FFF and DIW techniques. Each process parameter of the methodology is discussed. A DOE based experiments were performed and observations were analyzed for fabricating composite scaffolds using biodegradable materials PLLA and a newly developed radiopaque polymer Rylar.
- Chapter 4: The developed methodology was further investigated to print multilayer scaffolds and multiple tests were performed to address the challenges faced during previous experiments. This chapter recovers all the test that were performed to fabricate composite scaffolds with more number of layers of each material.

- Chapter 5: The results of developed methodology and its applications in fabricating multi-layered scaffolds are discussed in this section.
- Chapter 6: Conclusions and recommendations for future research.

CHAPTER 2

Custom Multi-Modality 3D Bioprinter

2.1 Additive Manufacturing Definition

Additive Manufacturing also known as 3D printing is a process where material is added layer by layer to build a 3D structure instead of subtracting the material. A holistic approach of AM is represented in figure 2.1. A design file or CAD file is created and converted to .stl file. .stl file is sliced into G-codes using open source software like Slic3r (GNU Affero General Public License) and Cura (Ultimaker, Netherlands). It is a process where CAD file model is approximated by triangles when .stl format is used [38]. G-codes are sent to processors such as Rumba board using open source software such as Repetier Host (Hot-World GmbH & Co., Germany). Implemented firmware on processor will process the G-codes and send the signals to AM platform, which will carry out the printing. In the end, the user has 3D printed built or structure. This research work uses an in-house 3D bio-printer developed at Micro Manufacturing Automation and Robotic Systems (MARS) lab.

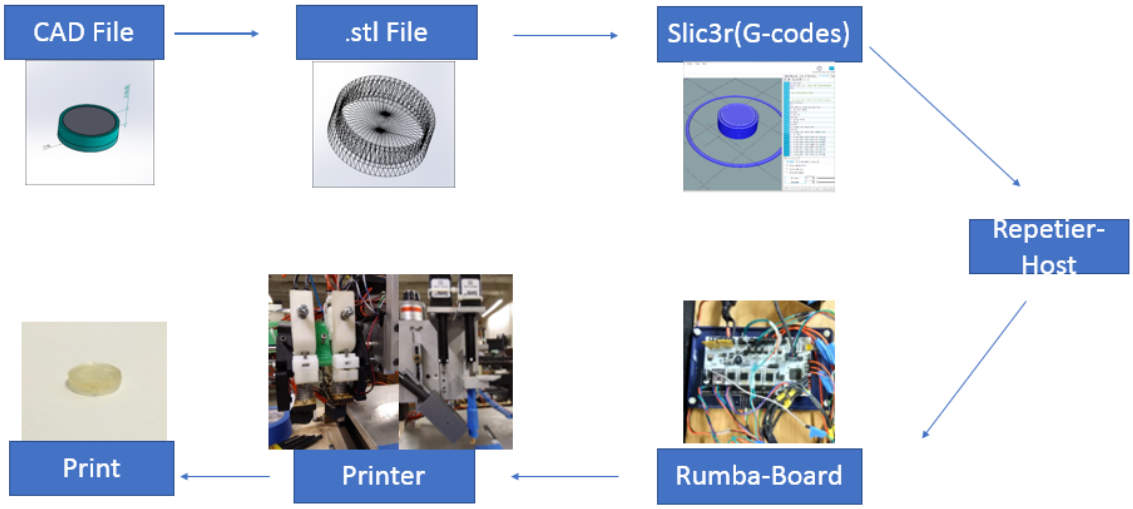

Figure 2.1: Holistic approach of Additive Manufacturing or 3D printing

2.2 Multi-Modality Bio-printer

Bio-printer is an essential technology for tissue engineering and organ printing [39] [40]. Commercially available bio-printers from envision-tec (`www.envisiontec.com/3d-printers/3d-bioplotter/`) and Organova (NovoGen MMX Bioprinter) are used by researchers for applications in tissue engineering [41]. These printers have limitations in terms of materials that can be processed and AM techniques used. CMMB (Custom Multi Modality Bioprinter) was developed to integrate existing AM techniques on a single platform [42]. In-house-built 3D bio printer is a XYZ based platform with modalities of Viscous Extrusion (VE) module, Inkjet Module (IJ), Fused Filament Fabrication (FFF), Direct Ink Writing (DIW) or Photo Polymerization Module (PP), and currently developed Pneumatic Module (PM). It has Marlin firmware based Rumba board as the processor and Repetier-Host as the host software. For this research work, three modalities FFF, DIW, and PM were used. Understanding of each modality is necessary to evaluate the effect of process parameters on 3D

printing. A detailed explanation of each module and open source software Slic3r are described in this section.

2.2.1 Fused Filament Fabrication Module

FFF module is a stepper motor based extrusion module where material in filament form is passed through a heater and a nozzle. Process parameters such as print speed (S), nozzle to bed distance (NBD), nozzle diameter (D), extrusion temperature (T), in-fill density, and in-fill pattern are user defined. Mechanical properties like flexural strength, surface roughness, strut geometry, and strut width are highly dependent on these process parameters [43] [44]. A controlled extrusion takes place where extrusion feed is correlated with speed of XY motion of the platform or print speed. CMMB 3D bio-printer has three FFF modules to process multi-material printing on a single platform in a single run. Two of current three FFF modules are represented in figure 2.2. One extruder has metal nozzle of 0.4 mm while another has 0.3 mm nozzle to print with different strut width. All the FFF modules can be independently calibrated along Z-axis.

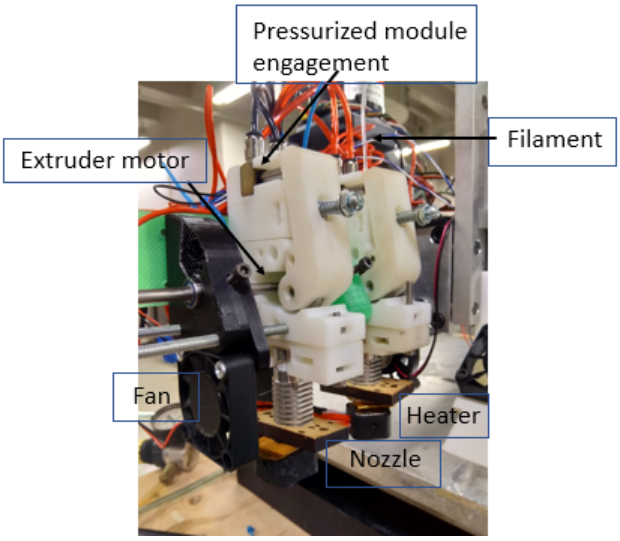

Figure 2.2: FFF module with its features

2.2.2 Viscous Extrusion Module

VE module is a syringe-plunger based extrusion module. A stepper motor pushes the plunger in syringe to extrude the material through a linear needle. It was developed to dispense viscous gel type of materials controllably. Extrusion takes places in very low volumes when 1/32 micro-stepping stepper drivers actuate linear motion of plunger. The module has also provision to be calibrated independently along Z- axis. A standard syringe of 15.75 mm inner diameter was used with 0.25 mm diameter Polytetrafluoroethylene (PTFE) flexible needle. Developed extrusion module is presented in figure 2.3. For the preliminary experiments, toothpaste was used as a viscous gel.

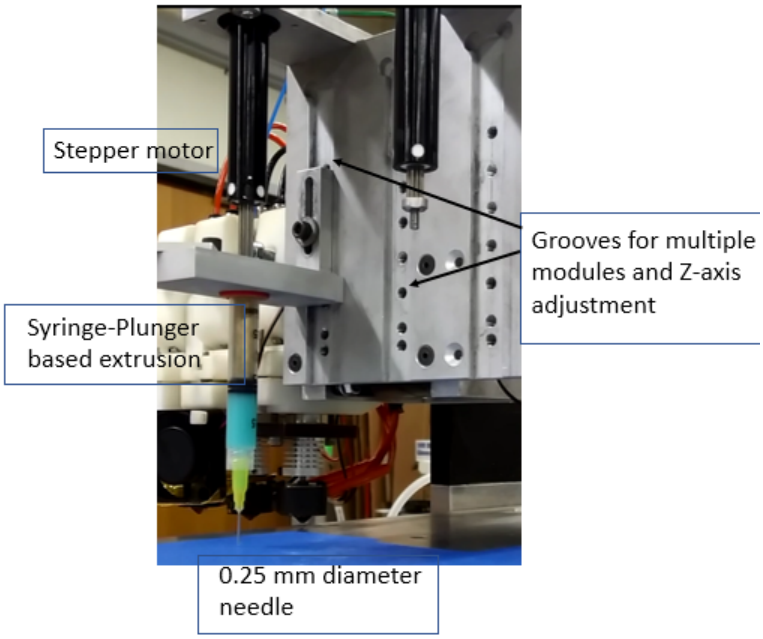

Figure 2.3: VE module with features

2.2.3 DIW/PP Module

Direct Ink Writing or Photo-Polymerization module was developed to dispense the photo-curable and cross-linking bio-materials using syringe-plunger base mechanism. David C. and Kimberly L. have explored advanced bio-inks, their feasibility for 3D printing and clinical use [45]. Ultraviolet (UV) source was integrated in module to photo-cure the dispensing material. As represented in figure, a stepper-motor based DIW module has 0.25 mm PTFE flexible needle and a UV light-guide attached to it at 45 degrees to cure the photo-curable dispensing material in-situ. A cap was designed and attached to the needle to avoid the direct flooding of UV on needle and clogging of the needle. Similar to other modules, it has provision to be calibrated along Z-axis independently. Here, BlueWave 75 (Version 2.0 UV) curing spot lamp is used as an UV source which is operated independently by the user.

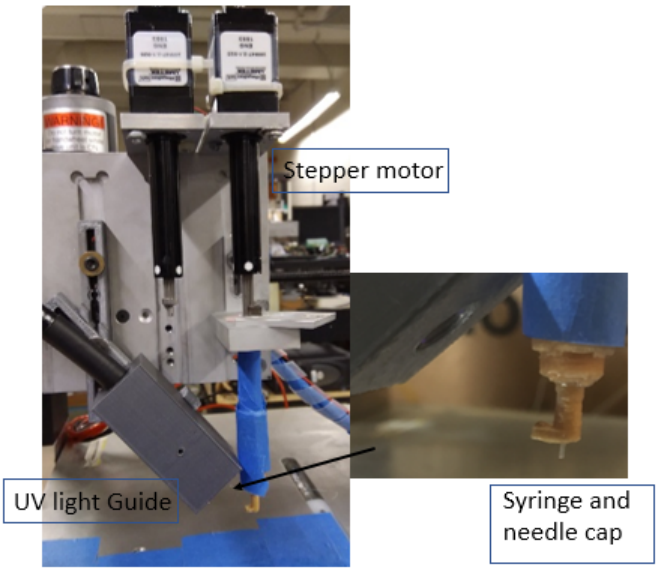

Figure 2.4: DIW module with features

2.2.4 Slic3r and Repetier Host

Slic3r is an open-source slicing software to convert CAD files into machine operation files. Certain file formats like .stl, .3mf and .amf are transformed into layer by layer addition of material. Pulak et al. has mentioned different slicing procedures for layered manufacturing [46]. An .stl file is an approximation of the surface of the CAD model using triangles. Slic3r takes the points of those triangles, convert them into a layer of the part, and define the extrusion based on process parameters. An user interface of Slic3r software has print settings, filament settings, and printer settings which allow to specify print parameters, filament dimensions and extrusion temperature, and hardware specifications of printer, respectively. A .stl file is placed at desired location on the bed and sliced to generate the G-codes for printing. Repetier Host is software to communicate between the processor and the computer. A manual control of printer is possible through Repetier-Host software. Also, it incorporates

post-processing of G-codes to facilitate adjustments in the printing process. Figure 2.5 represents the user interface of the Repetier-Host software.

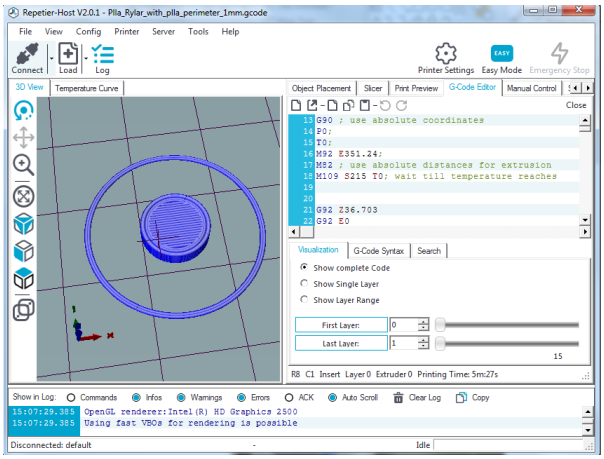

Figure 2.5: Graphical user interface of open-source software Slic3r and Repetier-host

2.3 Combination of FFF and DIW modules

The in-house 3D printer has unique capabilities to combine FFF and DIW modules. DIW module developed on printer is different than traditional stereolithography technique. It uses direct deposition of photo-curable material and the UV attached to it allows the in-situ curing of the material. In conventional stereolithography method, inverted or upward container is filled with photo-curable resin material. Light source is guided over the resin material to cure it and print single layer of the part. Then, the base plate is moved upwards or downwards to fill the resin material and print next layer. Conventional SLA technique requires resin material in large quantity to fill the vat. On the 3D printer developed at MARS Lab, optimum material can be utilized. Syringe based extrusion allows minimum use of resin. It satisfies the requirement and makes the printer design compact.

The unprecedented combination of FDM and DIW technologies allows the user to experiment with solid and liquid materials at the same time. Parts with heterogeneous structures can be built using this technology. Specifically, in tissue engineering where heterogeneous structures of human organs are fabricated using in-situ cell injection proliferation, this technology can be advantageously employed.

CHAPTER 3

Development of a 3D printing technique for the fabrication of the composite scaffolds

3.1 Characterization of the experiment

The experiments were designed considering human trachea. The basic idea was to evaluate the adherence between newly developed bio-resorbabale photocurable polymer, poly glycerol sebacate fumarate gadodiamide (Rylar) mixed with PEGDA (Poly ethylene glycol) diacrylate 50% wt/wt, and bio degradable polymer poly-L-lactic acid (PLLA). Since the Rylar mixed with PEGDA has elastic properties post curation, it can be used to create bio resorbable pipe like the trachea for the treatment of tracheomalacia. As these were preliminary experiments, proposed geometry had certain number of layers of each material. The 3D printed geometry using in-house built 3D printer is described in the following section.

3.2 Proposed geometry of the composite scaffold

A geometry of circular disc was selected for 3D printing as it resembles the geometry of human trachea. As these were preliminary runs, parts with smaller dimensions were printed to verify the proposed experiment. A hollow disk with 10mm outer diameter, 6mm inner diameter, and 0.8mm thickness was modeled using SolidWorks (Dassault Systmes Americas Corp., Waltham, MA, USA) and converted to the .stl (Standard Tessellation Language) file format. Here, a 0.4 mm base consist of PLLA and 0.4 mm of Rylar-PEGDA was printed on top of PLLA base. Figure 3.1 illustrates the design.

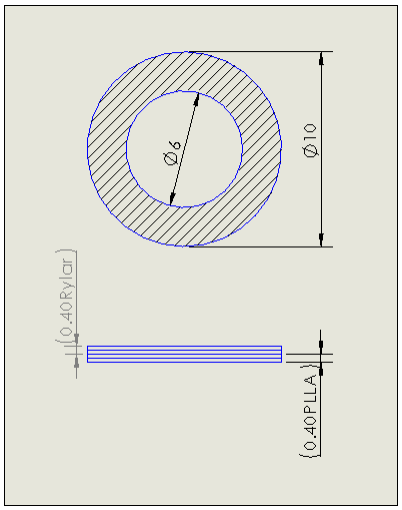

Figure 3.1: Proposed geometry of the composite scaffold

3.3 Materials

3.3.1 Rylar Synthesis and Material Preparation

Two-step synthesis from Deithyl Fumarate and Polypylene Glycol facilitated by Gagodiamide Anhydrous was carried out to produce Rylar[29]. Method for Rylar synthesis is described by Goodfriend et al. [29]. Rylar was mixed with photo curable PEGDA 50% wt/wt. Mechanical properties of 3D printed Rylar-PEGDA structures are reported by Ravi et al. [47].

3.3.2 PLLA Synthesis and Material

PLLA fibers of 1.55 $\pm$ 0.1 mm were extruded at 180-185 degrees centigrade from PL-32 granules. 4 stage melt extruder (ATRTorque Rheometer, Brabender, Hackensack, NJ, USA) was used to make the filament of PLLA.

3.4 3D Printing Methodology

In house built Custom Multi-Modality 3D bioprinter with FFF (Fused Filament Fabrication) module and DIW or PP (Photo Polymerization) module was used for fabricating samples [48]. FFF module and PP modules used are compatible with thermoplastic materials and photo curable viscous liquid, respectively. The process parameters used for PLLA were 100% fill density, concentric infill pattern and 0.2 mm layer height. The PLLA base was printed at a constant print speed of 600mm/min for all samples. Extrusion temperature for PLLA was set to 215 °C. Nozzle to Bed Distance was set at 0.2 mm. Rylar-PEGDA was printed on top of the 0.4 mm PLLA base using PP module. The thickness was again set at 0.4 mm (2 layers) with 80% infill, concentric infill pattern, 0.2 mm layer height and 0.25 mm extrusion width. G-codes were modified to build up pressure at beginning and avoid extrusion at the end as the extrusion vs feed profile is not linear for syringe-plunger based viscous extrusion. A 0.25 mm PTFE flexible needle was used to dispense Rylar-PEGDA. UV light with intensity 250 mW/cm^2 at syringe tip was calibrated for in-situ curing of the Rylar-PEGDA for all samples. Dymax ACCU-CALTM UV radiometer was used to measure the intensity of UV at syringe tip. 70% Isopropyl alcohol (distributed by Kroger CO.) and adhesive spray (TRESemme, Unilever) were used indirectly to prepare bed surface for every single run to make sure PLLA sticks to bed. PLLA only 0.4 mm thick disks were 3D printed as controls.

Three print speeds, 400mm/min, 500mm/min and 600mm/min were used for printing Rylar-PEGDA which led to curing time of 2 min 33 seconds, 2 min, and 1 min 42 seconds respectively. To avoid any bias in experiments, randomization of speeds was performed using List Randomizer (https://www.random.org/lists/) and implemented. Minimum of three samples for each print speed were printed. Print

speed is focused parameter in this research. Samples were air dried and weighed using a Sartorius precision balance (Pre-cision Weighing Balances, Bradford, MA).

Most of the parameters mentioned are discussed in detailed. It is necessary to comprehend the effect of each parameter in 3D printing to have thorough understanding of the technology and the methodology. The setup of CMMB is represented in figure 3.2.

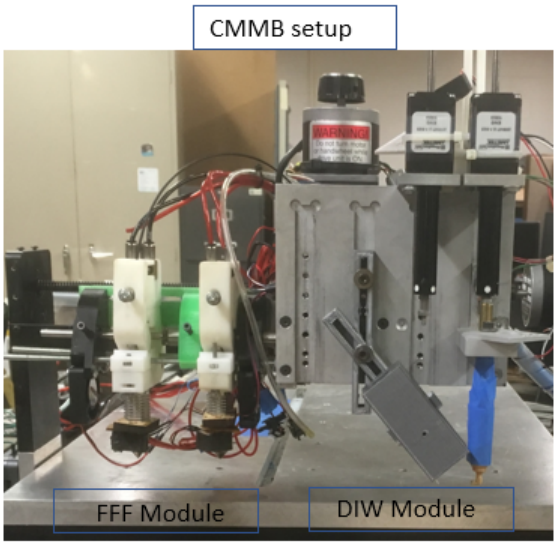

Figure 3.2: CMMB setup

3.4.1 Calibration of Z-axis

Calibration of Z-axis is necessary to correlate the software's understanding of Z-axis and physical location of Z-axis on XYZ platform. Layer height decided in the Slic3r file assumes that the extruder is physically at the same height what the G-codes are suggesting. For CMMB, the viscous extrusion module and FDM module have adjustable Z-height and one has to manually calibrate Z-axis. It is important that nozzles of both extruders remain at same level along Z-axis. First, Z-axis of

Photo-Polymerization module was calibrated, since it does not have set up to change Z-axis of needle once implemented. After that, Z-axis of FDM module was calibrated in way that both the nozzle tips were at same Z-height. Standard gages were used to measure the NBD between nozzle tip and bed surface.

3.4.2 Offset calibration between extruders along X and Y axes using ImageJ

Effective multi-material printing requires precise control of nozzle tips locations of different extruders. If the offset between two extruders are not properly measured, the printed part would have irregular geometry and bad print quality. Also, offset misjudgment can lead to nozzle striking already printed parts. An example of miscalculated offset is represented in figure 3.3. Figure 3.3 shows a printed part with a square using Poly Lactic Acid (PLA) base and a channel filled with toothpaste (viscous) material.

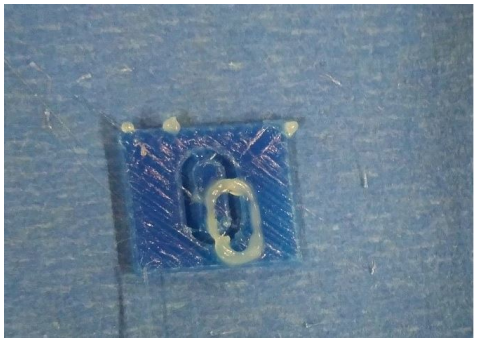

Figure 3.3: Multi-material printed part with miscalculated offset between extruders

For measuring offset between two extruders of CMMB, open source software ImageJ was used. ImageJ is a processing program designed for scientific multidimensional image (ImageJ, 2017). The software requires pre-placed physical standard scale while taking one image for calibration, from which decimal standards can be

converted to pixels. L shape part as represented in figure 3.4 was 3D printed by each extruder. A photo with a scale placed in the frame was processed in ImageJ to find the offset along X-axis and Y-axis.

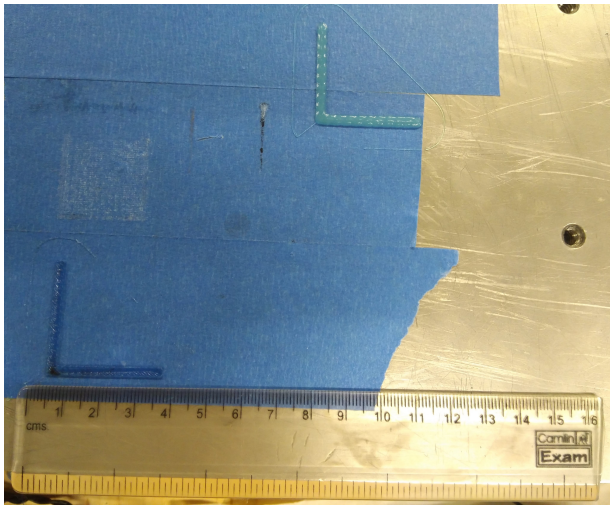

Figure 3.4: Offset calibration using L-shape 3D printed parts from two extruders.

After preliminary experiments to evaluate precise locations of the extruders, main experiments were performed. It was noted that X-axis offset was 76.50 mm and Y-axis offset was 203.45 mm. Every setup requires a new calibration and same trials were conducted with PLLA in FFF module and Rylar in Photo-Polymerization module. Manual adjustment through G-codes was also used to support the procedure.

3.4.3 Offset calibration between extruders along X and Y axes using user defined tool

A vision based user-defined tool was developed in-house by Tushar Saini to improve the calibration of offset between X and Y axes of PP and FFF modules. A web-cam based user-interface was implemented to view the nozzles of the different extruders from below. The calibration procedure was as follow: First the Z-axis of

both extruders were set at the same height using previously described method of Z-axis calibration. With the manual control mode in Repetier-Host, FDM module was placed at certain Z-height over the camera and nozzle's center point was located as represented in figure 3.5a. Once the values were noted, the location of the PTFE syringe of PP module was noted using same method as represented in figure 3.5b.

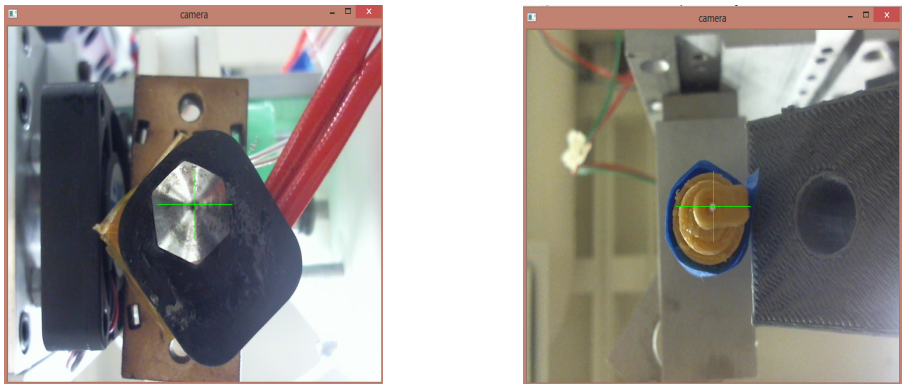

(a) FDM module in camera (b) PP module in camera

Figure 3.5: User interface view of extruders from bottom

An important parameter to consider while measuring the location is Z-height of both extruders for performing the calibration. A simple subtraction of noted values will give the offset between two extruders. Since feedback loop is not available in the system of calibration, print quality is the only way to evaluate the accuracy of the method. Since the procedure includes centering of plus sign on the nozzle, the maximum error in the calibration can be up to 0.25 mm (diameter of nozzle). To avoid such high error value, the precise centering of cross is necessary by user to get best results. A machine vision based system can be developed for self-calibration of print heads and better accuracy [49]. The user-interface of the developed tool is represented in figure 3.6.

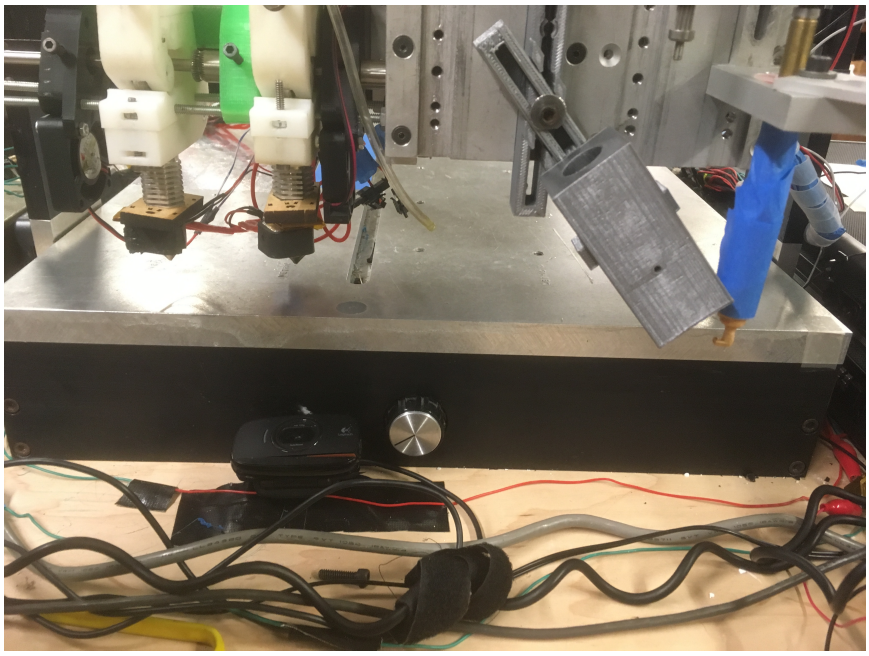

Figure 3.6: Setup for calibration

3.4.4 Nozzle to Bed Distance

Nozzle to Bed Distance is a parameter which decides the layer height of the printed part. Layer thickness has effectiveness of 49 % to 56 % on print quality [50]. Also, layer thickness decides processing time [51]. To high nozzle to bed distance will lead to extruding that just curls around the nozzle instead of sticking to bed. For this experiment, layer height of 0.2 mm was defined for each layer. For additive manufacturing, recommended NBD is 80% of nozzle diameter. The performed experiments had NBD less than or equal to 80% of nozzle diameter. To verify the recommended parameter value, PLLA was printed with 100% of NBD. Printed part is presented in figure 3.7a. A higher NBD led to bad print quality as shown in figure 3.7a. Also another parameter, bed surface, plays a major role in 3D printing. Extruding material should stick to bed surface for better print quality of first layer of the printed part. PLLA printed on smooth surface led to bad print quality as shown in figure 3.7b.

Effective print parameters are necessary to be evaluated in order to get required print quality as represented in figure 3.7.

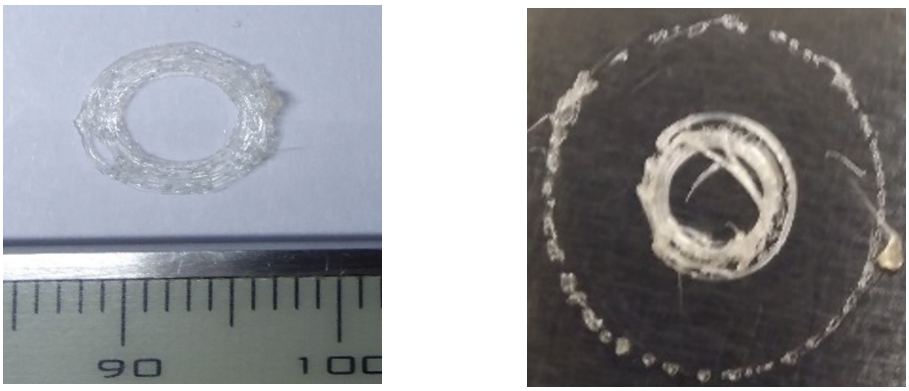

(a) Unsuccessful printing of PLLA due to higher NBD

(b) Unsuccessful print due to smooth bed surface

Figure 3.7: Effect of wrong print parameters on the quality of printing

3.4.5 Print Speed

Based on preliminary experiments, print speeds of 400mm/min, 500mm/min and 600mm/min were selected for the experiments. Print speed is the only varying parameter for DOE. As mentioned earlier, list randomizer was used to avoid any bias in the experiments. Importantly, print speed decides the duration of UV exposure that photo-curable resin receives. Table 3.1 provides exposure time for the samples with three different print speeds.

Table 3.1: Exposure time with respect to print speed

Print Speed (mm/min)	Exposure time (min:sec)
400	2:30
500	2:00
600	1:42

3.4.6 UV light intensity and calibration

PhotoPolymerization module has UV light lens which floods light on the tip of the nozzle. Knowing the value of UV intensity at the nozzle tip can help to evaluate the in-situ curing. The intensity of the UV at nozzle tip in the PP module should have minimum value of 100 mW/cm^2 to cure the Rylar in-situ. As per the inverse-square law, the intensity of UV light is inversely proportional to the square of the distance from the light source. A fixture setup designed by Dr. Prashanth Ravi for the Dymax Radiometer was used to calibrate the peak intensity of the UV light at nozzle tip. An indirect method was defined to measure the intensity on the detector and calibrate the UV intensity at the tip of the nozzle. First, fixture holding UV light guide is fixed in second most groove from the syringe (represented in figure 3.8), where light guide can flood light on the nozzle tip. Now, the fixture with light guide is moved to the adjacent groove and fixed precisely at the same height as earlier setup. Either pre-designed fixture or Vernier Caliper can be used in the grooves to make sure that fixture with light guide is fixed at same height as previous groove.

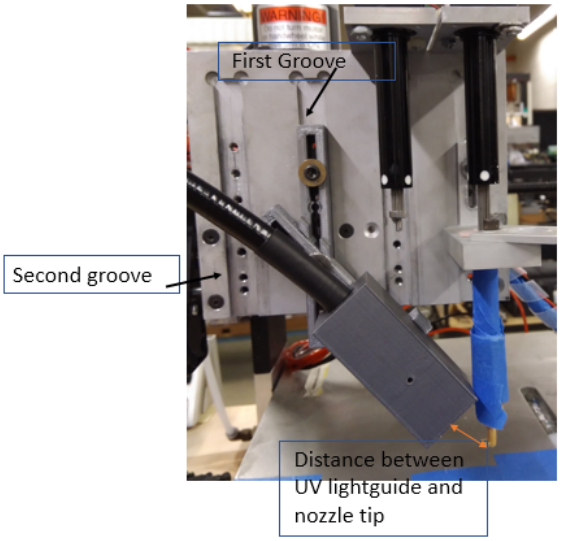

Figure 3.8: Fixture setup for UV light intensity calibration

Now, the detector of the radiometer is placed on the bed. The PP module is moved on XY platform manually such that the fixture with light guide will focus on the lens of the detector. The location on the print bed was X0 Y153. Simultaneously, the Z-axis of the PP module is lowered to a point where the gap between the bed and the nozzle tip is same as the height of the lens of the detector of the radiometer. Naked eye vision is used to make sure that the light guide focuses precisely on the detector which was 10.71 mm. The calibration technique gives the value of the peak intensity at the syringe tip. The UV light source is turned on and the desired peak intensity is adjusted on the UV source. Peak intensity of 250 mW/cm2 were used to cure the resin material for this experiment. After the peak intensity is calibrated, the fixture with light guide is replaced to the initial groove at the same height where it was focusing on the syringe tip. The distance between the nozzle tip and UV guide light was measured as 24.7 $\pm$ 0.1 mm. UV intensity calibration is required each time the user wants to change the intensity of curing, thus making it a tedious task.

A combination of process parameters is required for better control of dispensing and print quality during printing. UV intensity is needed to be correlated with print speed. Lesser UV intensity of 100 mW/cm ^{2} with print speed of 600 mm/min led to print of uncured Rylar as represented in figure 3.9. UV intensity received by Rylar was not enough to solidify which leads to spreading of fluid (Rylar) and eventually bed print quality.

Figure 3.9: Unsuccessful printing of Rylar due to lower UV intensity

3.4.7 Nozzle diameter

Nozzle diameter is an effective parameter in deciding the width of the strand. The width of the polymerized or fused deposited strand is directly proportional to the inner diameter of the nozzle. For these trials, nozzles of 0.4mm and 0.25mm PTFE for FFF module and PP module were used respectively. PP module or DIW module can also be used for direct cell writing process where cells are incorporated in manufacturing itself [52] [53] [54]. HepG2 Cell viability decreases with reducing nozzle size for DIW process as it mechanically damages cell membrane integrity [55]. Our experiments were restricted to polymeric material processing for the fabrication of scaffolds.

3.4.8 Slic3r and Repetier-Host customization

Open source Slic3r has limitations in terms of multi-material and multi-process 3D printing. To print two different parts with two different materials, it is required to slice the parts individually and merge the two G-code files. Also, post processing of the merged file is required to adjust the layer heights. Furthermore, Slic3r does not allow process parameters changes in a single run. Parts with different in-fill density and pattern can not be set up in Slic3r in a single sliced file. It is necessary to slice a part individually with required process parameters. Also, Slic3r is not customized to use two different processes in one run. Here, proposed composite scaffold design has a base to be printed with FFF while top to be printed with DIW technique. Preliminary experiments were carried out to address the issues discussed. For starters, two parts with different porosities and design were sliced individually for FFF technique only. Merged G-code file was pre-processed to work with single extruder but with different process parameters. Printed part had following process parameters:base with 60% infill density, top with 90% infill density. FFF print-head had 0.4 mm nozzle, layer height of 0.2 mm, Poly Lactic Acid (PLA) filament of 1.75 mm diameter, extrusion temperature of 190 °C, and print speed of 600 mm/min were used for printing with 45 degrees rectilinear infill. 3D printed component is shown in figure 3.10.

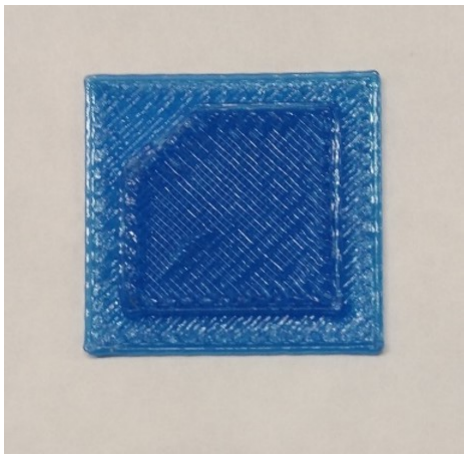

Figure 3.10: 3D print structure with single extruder but different fill density

3.5 Observations

Materials used have different properties; one in solid state and another in liquid state. For FFF, material that comes out of the nozzle depends on certain factors such as extruder temperature, viscosity of the material, surface tension, and shear force due to converging area at the nozzle entrance. It can not be predicted that there is a linear relation between extruding material and extrusion feed material. For good print quality, certain adjustments were made in the slic3r software and G-code were manually edited. First, two squirt loops were printed to get the continuous flow of material from the nozzle to avoid the discontinuity in the original part. Also, after every layer, it is necessary to retract the filament to avoid any unwanted extrusion, oozing, and blobbing. Though retraction changes the pressure in the nozzle, it is necessary for good print quality. The amount of retraction is usually decided by previous experience of the printer operator. For this particular experiments, a retraction of 3 mm was set in the Slic3r software.

Viscous Extrusion using stepper motor was used in Photo-Polymerization module for extruding Rylar. It is important to understand the difference between FFF

and VE. VE depends on factors like viscosity of the material, volume of the material, length of the nozzle/needle, and ratio of area of the nozzle to area of the syringe used. As extrusion in dispensing is a pressure dependent phenomenon, there is lag between the feed of the stepper motor and extrusion. It takes some time to build up the pressure and start extruding. Giving manual purge or printing squirt loop can solve the issue. Some retraction is also provided to avoid extrusion between layer-change. During the experiment, a manual purge of 0.05 mm before printing and adjusted 0.05 mm purge at the beginning of squirt loop were given. Also, to restrain the extra material coming out of the nozzle at the end of printing due to build up pressure, G-codes were manually edited to adjust retraction of 0.11 mm.

Bed surface plays a major role in additive manufacturing since print quality of the first layer of the part depends on it. Through-out the experimentation, 3M Scotch Blue Painters tape was selected as an adhesive surface. Alcohol and Hair Spray were used to clean the print surface before every run to make PLLA material to stick. It was observed that PLLA printed on new tape gives better print quality. While removing part from the surface, it leaves rough patches. If these rough patches are not smoothed using the hair spray, polymer particles from the next run will cling on the bed surface making it harder to remove. Alcohol was used to remove any remnants and dust particles before each run.

PLLA printing is mainly affected by NBD and filament temperature for the quality of the print. It was observed that even 83% of nozzle diameter of 0.30 mm for NBD lead to uneven print quality and layers were not sticking to each other. To improve the print quality and better surface finish, NBD of 67% of nozzle diameter was used. For attaining flat surface of each layer, layer height plays a major role.

Figure 3.11b represents a sample part of the composite scaffold. Figure 3.11a represents cross section of the composite.

(a) Continuously printed composite scaffold cross section

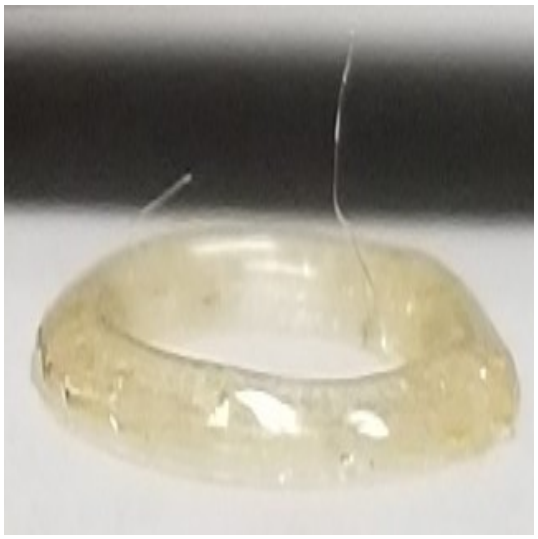

(b) Composite scaffold side view

Figure 3.11: Continuously printed composite scaffold

Samples weight had mean of 0.0276 g with standard deviation of 0.0023 g. That represents consistent 3D printing methodology. The weights of the parts are reported in Appendix table 1. The average inner diameter was found to be 5.70 mm and outer diameter was 10.05 mm.

CHAPTER 4

Fabrication of bio-degradable and bio-resorbable composite scaffold

4.1 Proposed geometry of composite scaffold

A circular composite module geometry was conceived during discussions with supervising professor Dr. Shiakolas and Dr. Welch. The proposed geometry is represented in figure 4.1. Previous experiments suggested successful development of the methodology to combine FFF and DIW technique for multi-material scaffold. New experiments are aimed at addressing the issues that were faced earlier. Modification in geometry of composite scaffold was performed to observe the effect of meniscus. Materials were sticking to each other when Rylar is printed on top of PLLA. Through new geometry, printing of PLLA on top of Rylar will be evaluated.

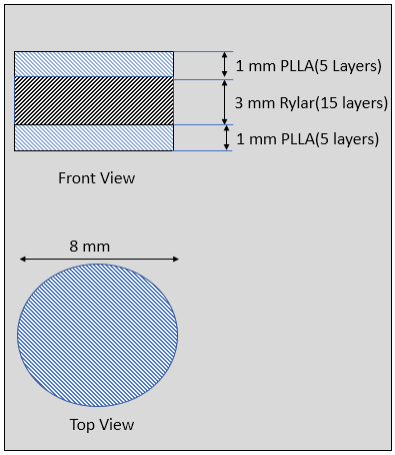

Figure 4.1: Proposed composite scaffold geometry

The idea is to 3D print an easily assembled small composite module from PLLA and PEGDA + PGSF (Rylar) which can be further assembled with similar modules

to make a structure like trachea. The design composes of 3 mm thick Rylar with 8 mm diameter is sandwiched between two 1 mm PLLA solids. Three parts were modeled in Solidworks (Dassault Systems American Corp.Waltham,MA,USA) and assembled. The assembly was saved as part in format of .SLDPRT file to differentiate the parts instead of merging them.

4.2 Slic3r and Repetier-Host customization for multi-material processing

Open source Slic3r and Repetier-host (Hot-World GmbH & Co. Germany) software is designed to operate on FFF printing only. Certain customization of settings in the software is necessary to enable it to work with multi-material and multi-process techniques. First, an .amf file was created from the .SLDPRT file. An .amf file allows to assign different extruders to different parts of assembly. The parts were combined in one group from the Settings section of software as represented in figures 4.2.

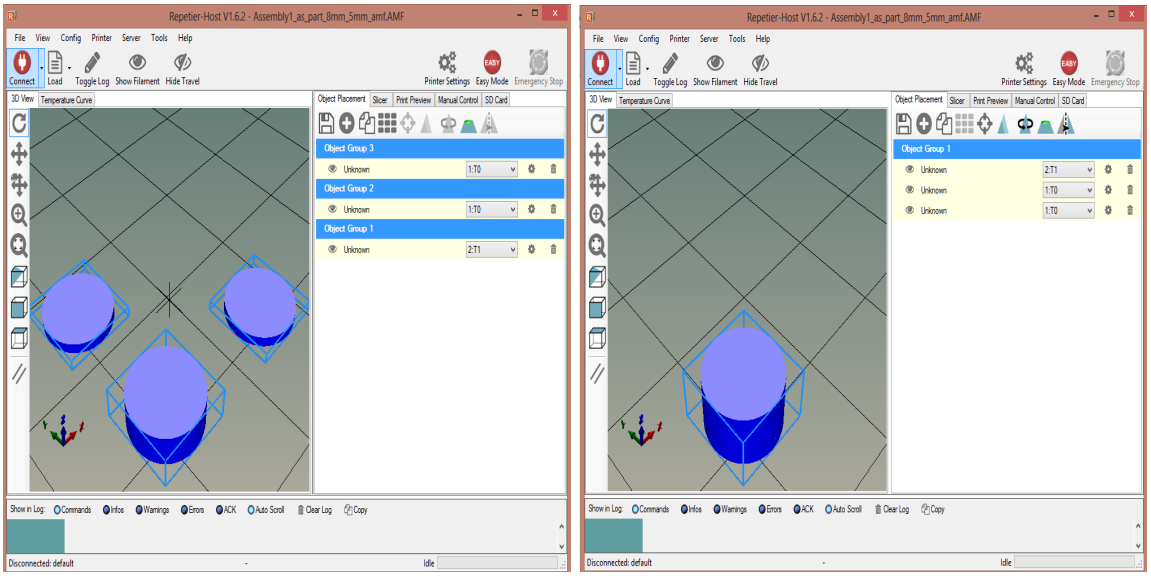

(a) .amf file with parts of assembly

(b) Assignment of extruders to different parts and their placement

Figure 4.2: Use of .amf file instead of .stl file

Sli3r has major limitation for multi-material and multi-process as it uses single set of print parameters through out the print. Print parameters such as layer height, fill density, and perimeters can not be changed in the same part. To include different print parameters in single run for multi-process and multi-material printing, merging of two sliced file is necessary. Slic3r file for PLLA printing has print parameters with print speed 600mm/min, infill-density of 90%, layer height of 0.2 mm and infill-angle of 0° with rectilinear infill while for Rylar-PEGDA layer height of 0.2 mm, infill-density of 68% and infill-angle of 0° with rectangle infill were selected based on preliminary experiments. Print speed and UV intensity for Rylar were the control parameters for experiments. Printer settings included two extruders and customized G-codes were written for starting, ending, and change between extruders. Post process of G-code file was done to include offset between two extruders and Z axis calibration.

4.3 3D Printing Methodology

Three different methodologies were tried to define the process and achieve the end results. For each set of runs, observations were taken and further changes were made in the next methodology. Understanding effect of print parameters on printed material can shade light on macro-level structure of the printed part.

4.4 Test 1: To observe the effect of print parameters and fluid property on composite scaffolds

The methodology described in section 3.4 with suggested changes in Slic3r as mentioned in section 4.2 were implemented for 3D printing of described geometry of composite scaffold. Print parameters for DOE are represented in table 4.1.

Table 4.1: Control Parameters

	PLLA	Rylar
Print Speed(mm/min)	600	600,400
UV intensity(mW/cm^2)	n/a	100

PLLA base was printed using 0.30 mm nozzle with layer height of 0.20 mm and infill density of 90% using FFF module with extrusion temperature set to 215 °C. Photo-curable Rylar + PEGDA was extruded using PP module with 0.25 PTFE flexible nozzle and 0.20 mm layer height. Since PP module has stepper based extrusion, initial purge and extrusion were manually encoded in G-codes to develop initial pressure. UV intensity was calibrated at nozzle tip and the measured distance from UV light-guide lens to tip was 24.5 ± 0.5 mm. Here, print speed is a research parameter which has a strong relation on mechanical properties of Rylar [47]. Print speed for PLLA was fixed of 600mm/min for reducing the overall print time. Print Based on preliminary experiments, UV intensity at nozzle tip was selected to be of 100 mW/cm^2. Fixture setup for UV light guide were kept in same position as described same as in earlier section.

4.4.1 Composite scaffolds with meniscus on Top

Printed composite scaffold as a result is represented in figure 4.3.

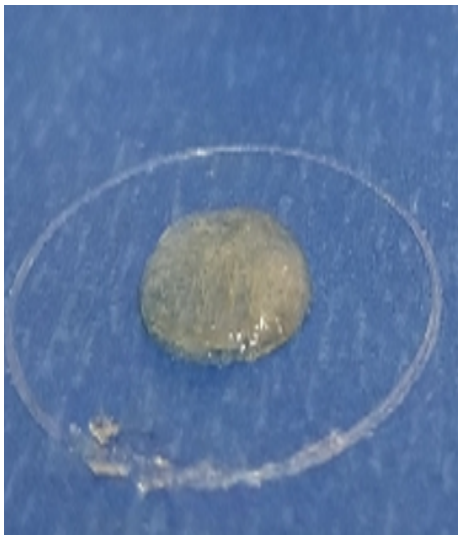

(a) Composite scaffold

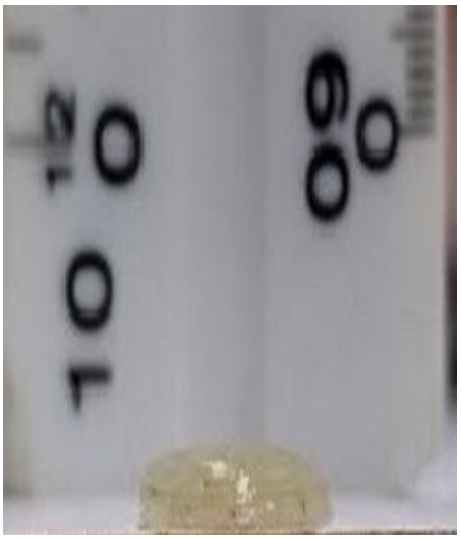

(b) Side view of scaffold design

Figure 4.3: Composite scaffold with meniscus on top

As shown in figure 4.3, the current set of print parameters, fixture setup and fluid property allowed only 1mm printing of Rylar. 3D printing of fluid generates a meniscus based on the viscous property of the fluid. Fluid with less viscosity tends to spread, while printing a strand and fluid with high viscosity will create larger meniscus due to high surface tension. Also, the surface roughness plays an important role in final print. With current setup, the material (Rylar) that is being dispense remains in liquid state instead of partially or completely solidifying. That allows materials to sag and get shape of curvature instead of flat surface.

Use of stepper based extrusion module leads to delayed extrusion, oozing of the liquid after the printing and unavailability of instant start-stop of extrusion during layer change. A certain pressure development inside the syringe is required for extrusion to happen. Since, continues linear movement of plunger will take some time to generate uniform pressure at the beginning of printing, a delayed extrusion occurs. At the end of the printing, developed pressure will lead to oozing or extra extru-

sion. That can lead to bad print quality and unnecessary inflated part. Also, stepper based extrusion module does not allow instant start-stop of the dispensing. This phenomenon has adverse effect on extrusion during layer change, where extrusion is needed to be stopped completely to avoid oozing of the extrusion. The FFF technique incorporates the retraction of filament to avoid oozing during layer change. Stepper based extrusion module can be retracted, but developed pressure is still present which cause extrusion.

4.4.2 Observation of the composite scaffold and modification in experiment

The issue of meniscus needs to be addressed to print multilayer structure along Z-axis using Rylar. Also, delayed extrusion can lead to improper distribution of material and eventually leading to uneven surface. After five layers of printing (1 mm) of Rylar, it was observed that dispensing but not controlled printing of material for the perimeter was moving along the PTFE nozzle. That created a channel for liquid flow and the Rylar started to collect at nozzle cap. This phenomenon is presented in figure 4.4. The collected material at the cap of syringe was polymerized, further increasing the chance of nozzle clogging. Also, used PTFE nozzle is flexible and has clearance in the syringe cap. A slight disturbance can lead to change in location of the nozzle tip. Dispensed but not cured photo-curable material can completely solidify at the nozzle tip. This can lead to change in location of nozzle tip with respect to the other nozzle. The overall effect can lead to change in X-Y axis offset between two extruders.

Figure 4.4: Dispensed but not printed material moving to syringe cap

In summary, a flat surface is required for continuous printing along Z axis. Further investigation is needed to address the issue of meniscus which can allow to print flat surface along the Z axis. Further experiments were carried out to address the limitations identified in Test 1.

4.5 Test 2: To observe the effect of reduced NBD on meniscus

Understanding of fluid behavior is necessary to reduce the meniscus. Here, with current setup of UV light-guide and syringe cap, the photo-curable Rylar is not instantly solidifying as it comes out of the nozzle. Being a non-Newtonian fluid [29], the viscosity of the Rylar changes as the pressure inside the syringe changes. As the material comes out of the nozzle, it will take the shape of a droplet because of surface tension and outside pressure. The liquid material will not maintain the shape of nozzle (filament) which can lead to poor structural integrity. For nozzle diameter of 0.250 mm, the chosen nozzle to bed distance of 0.200 mm will create a droplet at nozzle tip as represented in figure 4.5a. Suppressing the material as it comes out of

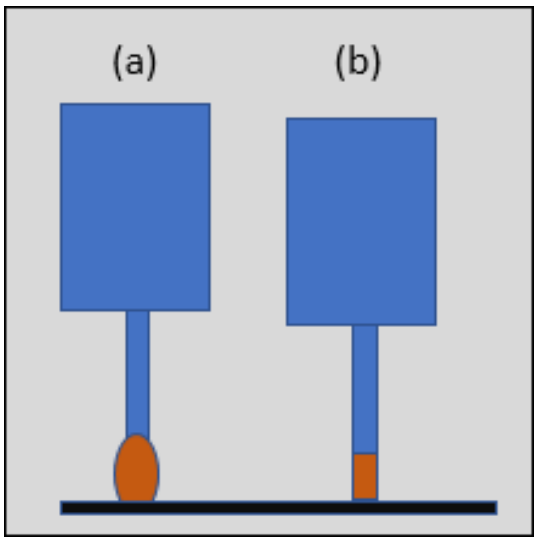

(a) Formation of droplet at nozzle tip vs desired shape

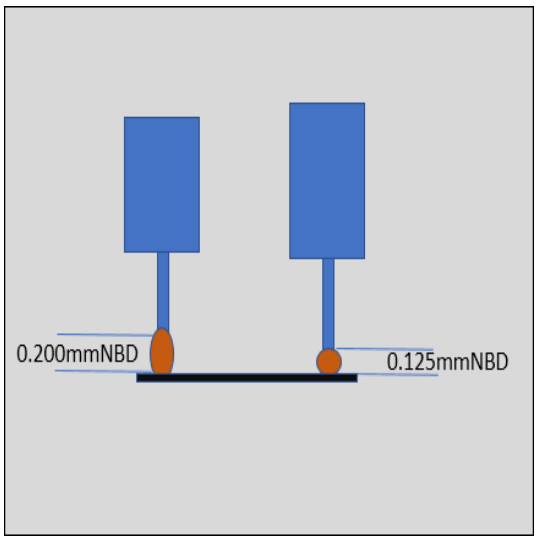

(b) Reduced NBD effect

Figure 4.5: Effect of change in NBD from 0.200 mm to 0.125 mm

the nozzle can flatten the surface of the liquid. For this set of experiment, nozzle to bed distance was kept half the diameter of nozzle. The effect of reduced NBD is schematically shown in figure 4.5. NBD was selected to be 0.125 mm instead of 0.200 mm. Total number of layers were doubled to achieve the overall height. This lead to twice the printing time for same print speeds.

4.5.1 Observation of samples for reduced NBD

The printed part is presented in figure 4.6. As observed, the meniscus on top still persists. Due to no instant solidification occurring at the tip of nozzle, the liquid spreads. A pin-point focus source could lead to instant solidification of liquid. Suppressing of material can have better surface finish at top if the material has high viscosity. Rylar mixed with PEGDA has apparent viscosity of 10,000-100,000

centipoise. With lower viscosity, the material does not maintain its shape after the extrusion and creates a meniscus.

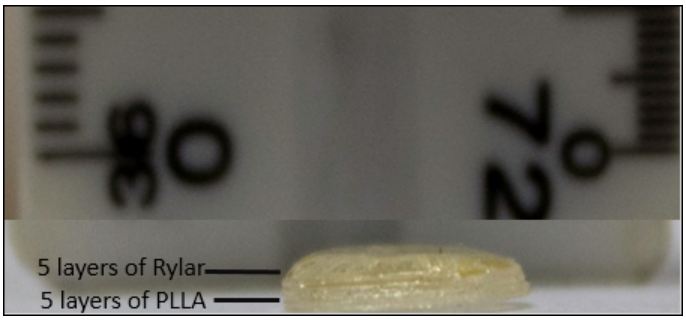

Figure 4.6: Composite scaffold with 0.125 mm NBD

4.6 Test 3: To address the issue of meniscus and limited vertical printing

In this set of experiments, preliminary experimentation was implemented with Rylar material only. The objective of the experiments was to observe the effect of different print speed and UV intensity. The final solidified perimeter of the part was then analyzed. Experiments lead to the conclusion that print speed of 250 mm/min with the UV intensity of 100 mW/cm^2 can generate partially solidified perimeter. The aim for this test is to be able to generate partially solidified perimeters. The partially cured perimeter can restrict the flow of liquid spread and flatten the surface. Through out the experiment, perimeter was printed at speed of 250 mm/min while other parameters were kept constant.

Also, the issue discussed in section 4.4.2 relating to material moving along the nozzle tip was addressed. Since the clearance between nozzle tip and syringe cap was increased.

4.7 Observation of composite scaffolds

The chosen set of parameters and fixture setup allowed fifteen layers of Rylar on top of five layers of PLLA which is required height of composite scaffolds. Four composite scaffolds had mean weight of 163.5 mg with standard deviation of 1.2 mg. Observation and recorded videos suggested that the issue discussed in section 4.4.2 of material being collected at cap was resolved. One of the composite scaffolds is presented in figure 4.7. A meniscus is still observed at the top instead of required flat surface. A success in terms of maximum number of layers of Rylar that can be 3D printed was achieved. Recorded video of a full printing cycle revealed an important phenomenon during printing. After 2 layers of printing, the perimeters will not have flat surface. Material that is dispensed but not printed will stay on the tip of nozzle until it finds the surface to print along the perimeters. The print continues once the extruder moves to in-fill printing.

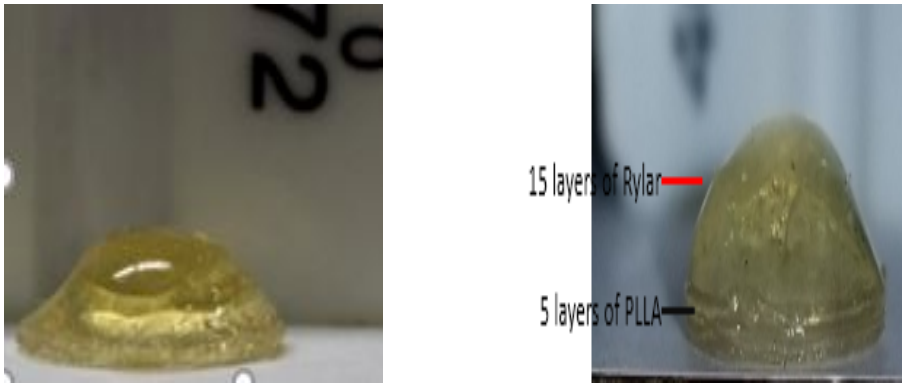

Figure 4.7: 1 mm PLLA with 3 mm Rylar Side View

4.8 Test 4: Composite scaffolds with PLLA perimeters around Rylar

Results from previous test indicate improvement in number of layers of Rylar that can be printed when partially solidified perimeters of Rylar are printed first. It

indicates that if a perimeter is solid enough to contain the flow then higher structure can be built with liquid. The concept with this experiment is to create a well where boundaries are built first and then in-fill is printed in same layer in later stages.

An assembly was designed in Solidworks with three parts: Circular solid base of 8 mm diameter with thickness of 1 mm, ring of 8 mm outer diameter and 7.2 mm inner diameter with thickness of 2 mm, circular solid part with 7 mm diameter and 2 mm thickness. The assembled part in Solidworks is presented in figure 4.8. Designed assembly was saved as .amf file. As mentioned earlier, .amf file allows to assemble the parts in Repetier software. Also, assigning of particular extruder to an individual part is possible. That way, the user does not have to merge two different files for combining two different technologies. Assembly was placed at desired bed location. FFF extruder was assigned to solid base and ring while PP/DIW module was assigned to inner solid as represented in figure 4.8. To have different process parameters for PLLA and Rylar, the assembly is needed to be sliced twice with required process parameters for each material. Then sliced files are merged to create a single file. G-codes were analyzed and it was observed that when combining two extruders in single layer, it will first print one layer with one extruder and then print two layers with another extruders. This can help to minimize meniscus. First, base of 1 mm thick PLLA is printed with one perimeter of PLLA on top. Then two layers of Rylar are printed. Since, the first layer of Rylar has solid boundary of PLLA, a concave meniscus will be generated. In second layer of Rylar printing, since there is no boundary available for printing, convex meniscus will be created. So eventually a flat surface can be expected.

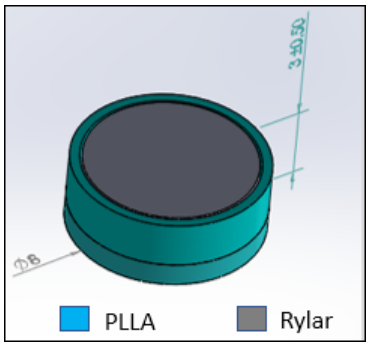

Figure 4.8: Assembled part with PLLA perimeter

A set of experiments was carried out in control environment using process parameters used in previous experiment. The observations are discussed in following section.

4.8.1 Observation of composite scaffold with PLLA perimeter around Rylar

A seamless integration between two extruders is required to have multi-material printing in single layer. An SEM image of a printed scaffold is presented in figure 4.9a. A meniscus was observed after 8 layers of Rylar. The overall printing was completed up-to height of 2.8 mm. The meniscus on top restricted further printing. Figure 4.9 shows a comparison between composite scaffold with 15 layers of Rylar on top and 8 layers of Rylar with PLLA boundary around it.

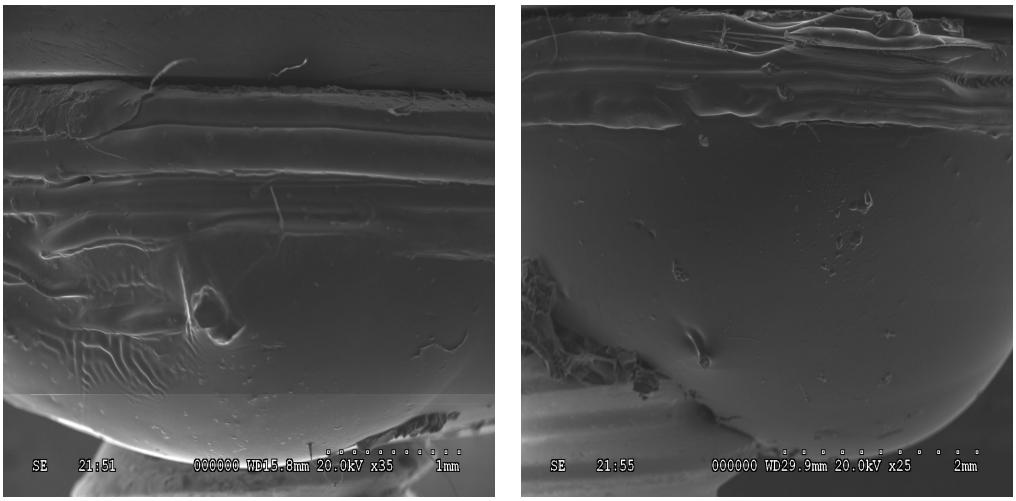

(a) SEM image of scaffold with solid PLLA perimeter

(b) SEM image of scaffold with partially solidified Rylar perimeter

Figure 4.9: SEM images comparison between perimeter of PLLA vs perimeter of Rylar

4.9 Test 5: To address the issue of delayed extrusion and oozing using Pneumatic dispensing

A stepper motor based PP module has limitations in terms of instant start-stop and delayed extrusion. A newly in-house developed pneumatic module was used to address the issue. The pneumatic extrusion module is an integral part of the multi-modality 3D printer. It can be combined with other modalities to incorporate multi-material multi-process methodology. For this research purpose, pneumatic module was used as a single modality. Focus of this test was to observe the effect of pneumatic dispensing on meniscus. The research work included only working with Rylar. The developed pneumatic module has Artificial Neural Network based pressure prediction for NEA123T material [56].

4.9.1 Methodology for 3D printing using Pneumatic based extrusion

Pneumatic based extrusion is related to pressure, diameter of syringe, apparent viscosity, nozzle diameter and nozzle length. Pneumatic extrusion allows instant-start and stop of dispensing. The pneumatic module was developed in-house using Nordson (Nordson Corporation, Westlake, OH, USA) pressure syringe and plunger, linear pneumatic control valve (Proportion Air Inc., represented in figure 4.10b), and a metal needle. A LabVIEW (National Instruments, Austin, TX) based user-interface connected with My-RIO micro-controller (National Instruments, Austin, TX) was developed to evaluate the extrusion feed for a print speed from stepper motor controller of Rumba-board. Utilization of stepper-motor controller from Rumba-board enabled researchers to develop and integrate module on same 3D printer. Developed LabVIEW VI uses G-code file provided to Rumba-board to find the value of extrusion feed for different print speed. Then the extrusion feed is characterized to estimate the pressure value to provide to the syringe using pneumatic valve. The correlated extrusion feed for desired print speed and calculations are performed using FPGA controller to avoid delay in extrusion.

A characterization of the flow is necessary to define the flow rate coming out of the nozzle in terms of described parameters. Based on characterization performed on NEA123T, preliminary experiments were carried out for Rylar. Nordson metal nozzle with diameter of 0.250 mm and 1 inch length was used in PP module for dispensing Rylar. The UV intensity at nozzle tip was 100 mW/cm^2. Preliminary experiments were carried out to relate different pressure to print speeds. For conventional 3D printing, extrusion feed is related to print speed using firmware and processor, in our case which are Marlin and Rumba board. When print speed is increased, extrusion feed is also increased and vice-versa. Since newly developed pneumatic module is

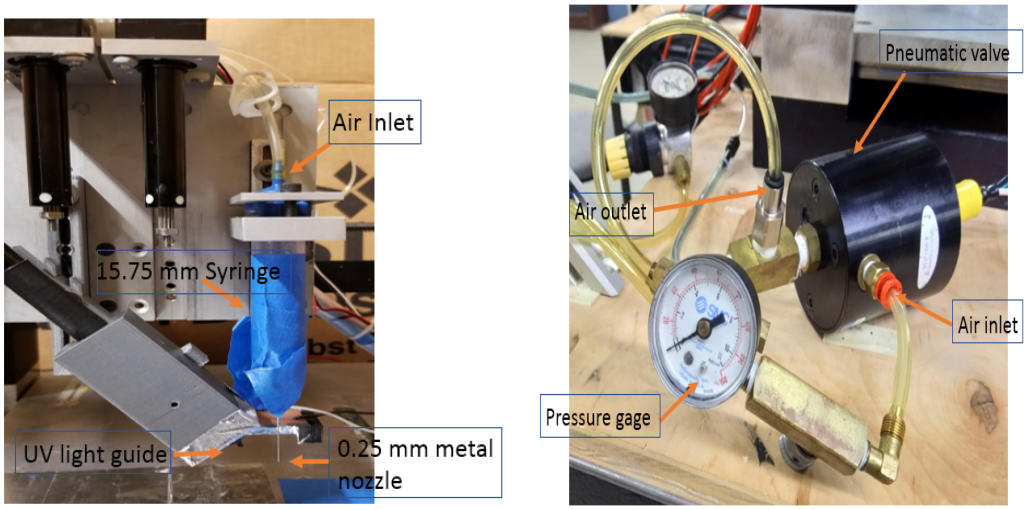

(a) Components of pneumatic module (b) Pneumatic valve

Figure 4.10: Pneumatic extrusion module

not customized for Rylar, experiments were carried out in controlled environment to estimate pressure for different print speeds.

Based on previous results, print speed (250 mm/min), UV intensity (100 mW/cm^2), and fill-density (70%) were kept constant to evaluate the pressure value. The preliminary experiments suggested pressure of 2.5 psi for these parameters. Circular and rectilinear patterns were evaluated to observe the effect of fill pattern on meniscus. The distribution of fluid while dispensing can lead to sagging in different directions, which may lead to reduced meniscus. Figure 4.10a shows the pneumatic print head on 3D printer. The experiments were setup in two sets, dividing them in circular infill and rectilinear infill.

4.9.2 Observation of Rylar scaffold

A better control of dispensing is available because of instant start-stop. At the beginning of printing, air is provided in syringe to initiate extrusion. Unlike plunger-syringe based extrusion, constant available air pressure starts extrusion with negligible

delay. During layer change, the low-input signal to pressure valve will stop air supply and remove the air inside syringe from exhaust valve (pressure release valve) to avail instant stop of dispensing. Oozing and delayed extrusion were minimized to accepted level using pneumatic dispensing.

Printed scaffold is presented in figure 4.11. Meniscus is still observed in scaffold of Rylar. Both circular and rectilinear infill pattern had similar results in terms of meniscus. Five layers with each layer of 0.2 mm and overall height of 1 mm were 3D printed. Also, after five layers of printing, dispensed but not printed material moves along the nozzle tip which restricted further printing. A PTFE syringe is recommended for future use instead of metal syringe to address the described issue. Two layers of printing did not have any issue. From third layer, meniscus restricted printing on perimeters.

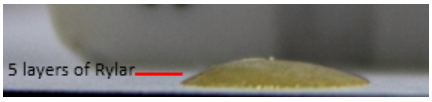

Figure 4.11: Rylar scaffold using pneumatic module

4.10 Test 6: Use of two in-situ UV sources to instantly solidify Rylar

An instant solidification of extrusion as it dispensed on bed may restrict the sagging of Rylar. A coherent and focused UV source at nozzle tip can avail such feature. For this set of experiments, a pin-hole projection was created at the UV-light guide. Another UV source, a UV LED, was incorporated in pneumatic extrusion module. The UV LED was set at 8 mm offset for curing Rylar. The concept here is to instantly photo-cure Rylar as it is dispensed using UV light projected through pin-hole projection at dispensing fluid and use another UV source to cure Rylar in-situ. A setup for the experiment is represented in figure 4.12.

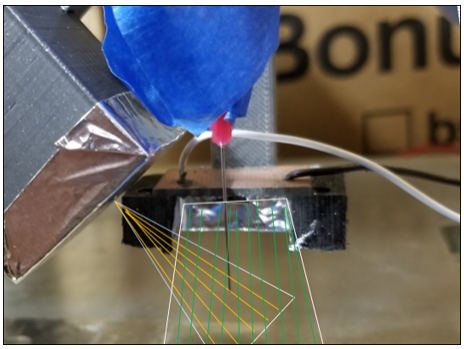

Figure 4.12: Setup of two in-situ UV sources for pneumatic extrusion module

4.10.1 Observation of printing

The calibrated UV intensity at nozzle tip was 80 mW/cm^2. The setup of two UV sources plays a major role in available UV intensity at nozzle tip. The current set of pin-hole projection is limiting the overall UV light that can enter through the pin-hole from light guide which is further reduced by diffraction through hole. UV intensity of 80 mW/cm^2 is not enough to photocure and solidify Rylar in-situ.

Modifications were implemented in the size of pin-hole to avail more UV intensity. With pin-hole projection removed, total UV intensity of 400 mW/cm^2 was achievable. Also, nozzle cap was removed to facilitate more UV intensity at nozzle tip. The remaining print parameters were kept constant and experiments were performed in controlled environment.

With low intensity of 80 mW/cm^2, Rylar was not solidifying at required rate. Uncured material kept sagging and restricting printing after 3 layers of printing. With UV intensity increased to 400 mW/cm^2, the nozzle clogged due to direct exposure of UV at nozzle tip. Photo-curable material Rylar has chain polymerization with photon curing. Since the cap was removed, the material being dispensed receives UV directly at nozzle tip. Chain propagation in the nozzle due to continuity and direct exposure to UV light can be the reasons for clogging.

The observations and results from printed parts suggest requirements of a focused UV source at dispensed material rather than at nozzle tip. A fixture development for focused UV source could be implemented to achieve the described concept.

4.11 Composite scaffold with PLLA-Rylar-PLLA structure

Proposed geometry included three layers of material in the structure with Rylar sandwiched between two PLLA plates. To investigate the possibility of PLLA sticking to Rylar, results from all previous tests were considered. Based on previous results, a similar geometry with less number of layers was conceived. From test 1 to test 3, it was observed that five layers of Rylar can be 3D printed with nearly flat surface on top of five layers of PLLA. After five layers of Rylar printing, meniscus will restrict the printing along the perimeters. For this set of experiments, only one layer of PLLA without perimeter on top of Rylar was considered for printing. The aim of the experiment was to give proof of concept of multi-layered composite structure, which included five layers of PLLA, five layers of Rylar, and one layer of PLLA without perimeters from bottom to top. The conceived geometry of the composite scaffold is represented in figure 4.13 .

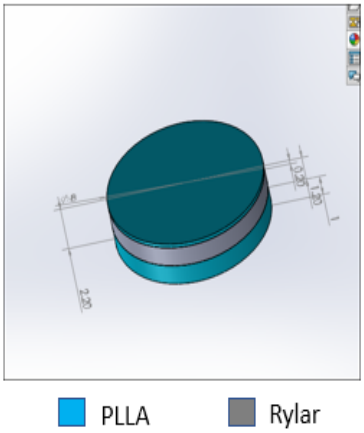

Figure 4.13: Proposed geometry of three layered scaffold

Design of experiment was carried out to avoid bias in the experiments. The combination of FFF module and DIW module was used to fabricate composite scaffolds. Process parameters were kept similar to test 3 because it had most success with respect to number of Rylar layers that can be 3D printed. Methodology described for test 3 was used to 3D print composite scaffold. G-codes file was prepared using .amf file where assembly was sliced twice to incorporate different process parameters for each AM technique. Adherence between two surfaces highly depends on the surface roughness of each surface. When Rylar is printed on PLLA, it finds gape between two adjacent threads which can improve bonding between two materials. As one can clearly notice from SEM images represented in figure 4.9 that Rylar does not print in struts. It has continuous material unlike PLLA. Also, it was observed that Rylar had relatively smoother surface finish than PLLA. To address these issues, PLLA filament was extruded at higher temperature of 220 °C.

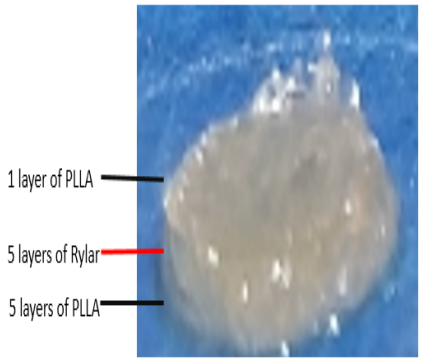

Figure 4.14: Composite scaffold with PLLA-Rylar-PLLA

4.11.1 Observations of three layered composite scaffold

The experiments were carried out in controlled environment. It was observed that higher PLLA temperature can be helpful to increase bonding between two material, specially when PLLA is extruded on top of Rylar. Recommended temperature range for PLLA is 180 °C - 220 °C. A higher temperature than 220 °C led to bad print quality for PLLA since the extruding material was in more liquid form rather than semi-solid state. A lower temperature than 180 °C leads to resistance in extrusion while higher temperature leads to extrusion with lower viscosity. Similar trends were observed with PLA printing by Ravi [43]. The resulted composite scaffold is represented in figure 4.14. One layer of PLLA was sticking to Rylar. The bonding between the two materials is enough to build more layers of PLLA. The meniscus prevents from printing perimeters on top of Rylar.

It was observed that seamless integration of two different techniques is possible. Also, no support structure was needed to build the composite scaffold even with three different parts.

4.12 Summary

A new geometry was proposed to address the challenges faced while developing the methodology for the fabrication of multi-material scaffold. To address the limitations of Slic3r, .amf file was used instead of .stl file. Though an .amf file allowed to assign different extruders to different parts, the assembly was sliced twice to get different process parameters for FFF and DIW techniques. Further, different sets of experiments were carried out to observe the meniscus created by Rylar. Investigation of process parameters and fixture setup were performed to increase the number of layers of Rylar. Overall fifteen layers of Rylar were 3D printed on top of five layers of PLLA with undesired curvature at the top. Observed issue of delayed extrusion and oozing in DIW module were resolved by the use of pneumatic extrusion module for the printing of viscous Rylar. A multi-layered structure with cylindrical Rylar solid between PLLA solids were successfully printed.

CHAPTER 5

Results and Discussion

5.1 Results of developed methodology of fabrication

Printed composite scaffolds exemplify that two materials stick together. Design of experiments (DOE) results for mean weight suggests a consistent methodology for 3D printing composite scaffold for two different materials with different properties and physical states. The characterized 3D printing technique can be used as basics to research the manufacture of a scaffold resembling human trachea. While PLLA material provides base and strength to the scaffold, PEGDA-Rylar works as elastic material to facilitate function of trachea. Also, printed parts exemplifies a 3D printing method for multi-material printing using photo-polymerization module and FFF module which are the most used techniques in today's 3D printers.

Challenges faced during the experiments suggested further investigation requirement in the area of multi-material and multi-process printing with respect to Slic3r customization. Furthermore, observed meniscus on top of scaffold due to viscous property of Rylar can restrict the maximum number of layers of Rylar that can be 3D printed. Overall, the developed technique's approach can be further researched to verify whether PLLA will stick on top of Rylar. Previous research performed on Rylar suggested strong correlation between print speed and UV intensity on elastic modulus of printed Rylar. Elastic modulus will decide the compressive strength of composite structure. Effects of print speed and UV intensity are needed to be studied on composite structure as well.

5.2 Results of solid composite scaffolds

A design of experiment (DOE) setup required preliminary experiments with Rylar which had photo-initiator added to reduce curing time. A controlled set of experiments based on DOE was carried out to address the challenges faced in methodology development. Results from printed parts suggested investigation of meniscus as the printing was reduced to overall height of 10 layers with 5 layers of Rylar printed on top of 5 layers of PLLA. To achieve the desired combination of multi-material printing, limitations of open source slicing software were addressed. The results open up many challenges in form of controlled dispensing of fluid, formulation of a meniscus due to viscous property of material, and restriction in vertical printing.

Experiments carried out by reducing the NBD did not give desired results in terms of overall height of printing, but the results further reinforced the effect of fluid property of Rylar on meniscus. Effect of more viscous fluid to gain the shape of filament while extruding can be investigated to get desired flat surface on top of composite scaffold.

Understanding of process parameters led to printing of 15 layers of Rylar on top of 5 layers of PLLA. A concept of creating partially solidified Rylar boundary helped to create higher structure for Rylar. Here, this test indicates the importance of fathoming process of in-situ curing. A correlation between a specific print speed (250 mm/min) and UV intensity (100 mW/cm^2) led to creating a partially solidified boundary. The concept of creating a well to restrict the flow worked in positive manner. Also, change in fixture setup avoided concentration of Rylar around the extruder nozzle. Again, positive results of overall layers had corroboration of mean weight for consistent printing methodology. A high resolution video of printing gave insightful information than a naked eye observation. Limitations of stepper-motor based ex-

trusion with unavailability of instant-start stop, delayed extrusion, and oozing were clearly observed. The positive results for overall height still need improvements in terms of better control of dispensing. Moreover, meniscus on top of composite scaffold prevents from getting desired flat surface. An investigation with solid boundary of PLLA gave similar results for overall height of composite scaffold.

In further investigation, delayed extrusion, oozing, and unavailability of instant start-stop was minimized through integration of Pneumatic based dispensing. Results from those set of experiments explain the fact that observed meniscus is due to viscous property of fluid as most of the challenges faced were minimized through sequential set of experiments. Rylar is less viscous which leads to spreading of liquid rather than maintaining its shape. Moreover, integration of two in-situ UV sources to instantly solidify extruding Rylar did not improve the results.

Composite scaffolds printed with three layered structure of PLLA-Rylar-PLLA had positive results. Materials sticked to each other while printing on top of each other. Though manual peeling revealed poor bonding strength at the Rylar-PLLA interface, bonding was good enough to carry out the 3D printing. Results clearly indicate that developed methodology for the fabrication of multi-layered composite scaffold is a possibility irrespective of sequence of printing of the material. Though meniscus on top of the Rylar prevents printing along perimeters, in-fill printing is feasible.

In summary, encouraging results were obtained with number of layers that can be printed using Rylar material. Test 1 to Test 6 results emphasize on meniscus being generated due to lower viscosity of Rylar and unavailability of focused source at extruding material instead of needle tip. Successful printing of multi-layered composite scaffold in a single run without any support structure represents an advantage of the developed methodology.

CHAPTER 6

Conclusions and recommendation for future research

6.1 Conclusions

Proposed geometry was aimed at developing a methodology to fabricate composite scaffold by integrating two different techniques of additive manufacturing, named Fused Filament Fabrication and Direct Ink Writing. The Research focused on using bio-degradable and bio-resorbable polymer materials, Poly-L-Lactic Acid in solid filament form and newly developed liquid radiopaque polymer PGSF (Rylar) mixed with PEGDA to fabricate composite scaffolds for the proposed treatment of tracheomalacia. The developed methodology with consistent results was successfully implemented in printing composite scaffolds. Further investigation addressed the limitations of open source slicing software for multi-materials and multi-process 3D printing technique. A number of experiments carried out to print more layers for the structure of composite scaffolds opened up plethora of concept development to address the challenge of meniscus. In the end, a multi-layered composite scaffold with Rylar being sandwiched between PLLA was successfully printed in a single run with multi-process technique without any support structure.

6.2 Recommendation for future research work

To advance the research, a detailed investigation needs be carried out to study the effect of increasing the viscosity of Rylar on the print quality. Higher viscosity of Rylar may enable the extruded material to maintain the shape of filament after extrusion, thus giving the desired flat surface. With that, a focused UV source pro-

jecting at extruding material rather than at needle tip can allow extruding Rylar to maintain its shape. A test, where partially solidified boundary around Rylar led to successful printing of 15 layers of Rylar, opens up a new concept of using a third compatible material to be printed as support perimeter. After printing the composite scaffold in a single run, third material can be removed by post-processing to get the desired composite scaffold of PLLA and Rylar. A proper investigation of bonding strength between the two materials is recommended through mechanical testing. Also, different fill patterns can be investigated to study the effect on meniscus.

Appendices

Table 1: Weight of the samples

	Weights(gms)		
Print Speeds(mm/min)	1	2	3
400	0.0308	0.0305	0.0277
600	0.0278	0.0253	0.026
600	0.0285	0.0291	0.024
500	0.0289	0.0268	0.0267
500	0.0231	0.0248	0.0256
400	0.0327	0.0298	0.028
600	0.0259	0.0242	0.0272
400	0.0292	0.0321	0.0287
500	0.0281	0.0277	0.0275

Table 2: Weight of PLLA samples

PLLA Only Print Speed is 600mm/min	Weights(gms)
1	0.0128
2	0.0122
3	0.0120
4	0.0135
5	0.0122

Bibliography

[1] M. Hoffman. Picture of the trachea. [Online]. Available: https://www.webmd.com/lung/picture-of-the-trachea#1,12/02/2017

[2] J. Flynt, "A detailed history of 3d printing," 2018.

[3] C. Hull, "Apparatus for production of three-dimensional objects by stereolithography," Mar. 11 1986, uS Patent 4,575,330. [Online]. Available: https://www.google.com/patents/US4575330

[4] D. H. Freedman, "Layer by layer," *Technology Review*, vol. 115, no. 1, pp. 50–53, 2012.

[5] C. R. Deckard, "Method and apparatus for producing parts by selective sintering," Sept. 5 1989, uS Patent 4,863,538.

[6] T. Wohlers, "Wohlers report," *Wohlers Associates Inc*, 2014.

[7] R. Jones, P. Haufe, E. Sells, P. Iravani, V. Olliver, C. Palmer, and A. Bowyer, "Reprap–the replicating rapid prototyper," *Robotica*, vol. 29, no. 1, pp. 177–191, 2011.

[8] D. Herzog, V. Seyda, E. Wycisk, and C. Emmelmann, "Additive manufacturing of metals," *Acta Materialia*, vol. 117, pp. 371–392, 2016.

[9] S. Solutions. Slm metal powder and machines. [Online]. Available: https://slm-solutions.com/products/accessories-and-consumables/slmr-metal-powder

[10] A. Atala, S. B. Bauer, S. Soker, J. J. Yoo, and A. B. Retik, "Tissue-engineered autologous bladders for patients needing cystoplasty," *The lancet*, vol. 367, no. 9518, pp. 1241–1246, 2006.

[11] J. Zuniga, D. Katsavelis, J. Peck, J. Stollberg, M. Petrykowski, A. Carson, and C. Fernandez, "Cyborg beast: a low-cost 3d-printed prosthetic hand for children with upper-limb differences," *BMC research notes*, vol. 8, no. 1, p. 10, 2015.

[12] B. Coxworth, "Scientists design potentially life-saving 3d-printed stethoscope," 2018.

[13] B. C. Gross, J. L. Erkal, S. Y. Lockwood, C. Chen, and D. M. Spence, "Evaluation of 3d printing and its potential impact on biotechnology and the chemical sciences," 2014.

[14] G. T. Klein, Y. Lu, and M. Y. Wang, "3d printing and neurosurgeryready for prime time?" *World neurosurgery*, vol. 80, no. 3, pp. 233–235, 2013.

[15] F. Rengier, A. Mehndiratta, H. Von Tengg-Kobligk, C. M. Zechmann, R. Unterhinninghofen, H.-U. Kauczor, and F. L. Giesel, "3d printing based on imaging data: review of medical applications," *International journal of computer assisted radiology and surgery*, vol. 5, no. 4, pp. 335–341, 2010.

[16] E. Mikołajewska, M. Macko, Ł. Ziarnecki, S. Stańczak, P. Kawalec, and D. Mikołajewski, "3d printing technologies in rehabilitation engineering," 2014.

[17] S. M. Peltola, F. P. Melchels, D. W. Grijpma, and M. Kellomäki, "A review of rapid prototyping techniques for tissue engineering purposes," *Annals of medicine*, vol. 40, no. 4, pp. 268–280, 2008.

[18] W.-Y. Yeong, C.-K. Chua, K.-F. Leong, and M. Chandrasekaran, "Rapid prototyping in tissue engineering: challenges and potential," *TRENDS in Biotechnology*, vol. 22, no. 12, pp. 643–652, 2004.

[19] V. J. Chen and P. X. Ma, "Nano-fibrous poly (l-lactic acid) scaffolds with interconnected spherical macropores," *Biomaterials*, vol. 25, no. 11, pp. 2065–2073, 2004.

[20] T. Lu, Y. Li, and T. Chen, "Techniques for fabrication and construction of three-dimensional scaffolds for tissue engineering," *International journal of nanomedicine*, vol. 8, p. 337, 2013.

[21] J. Phillip, "on the analysis of ceramic materials for the fabrication of biomedical scaffolds," 2016.

[22] M. M. Stevens, "Biomaterials for bone tissue engineering," *Materials today*,

vol. 11, no. 5, pp. 18–25, 2008.

[23] Z. Sheikh, S. Najeeb, Z. Khurshid, V. Verma, H. Rashid, and M. Glogauer, "Biodegradable materials for bone repair and tissue engineering applications," *Materials*, vol. 8, no. 9, pp. 5744–5794, 2015.

[24] Y.-C. Yeh, C. B. Highley, L. Ouyang, and J. A. Burdick, "3d printing of photocurable poly (glycerol sebacate) elastomers," *Biofabrication*, vol. 8, no. 4, p. 045004, 2016.

[25] E. MacDonald and R. Wicker, "Multiprocess 3d printing for increasing component functionality," *Science*, vol. 353, no. 6307, p. aaf2093, 2016.

[26] E. S. Bishop, S. Mostafa, M. Pakvasa, H. H. Luu, M. J. Lee, J. M. Wolf, G. A. Ameer, T.-C. He, and R. R. Reid, "3-d bioprinting technologies in tissue engineering and regenerative medicine: Current and future trends," *Genes & Diseases*, 2017.

[27] S. V. Murphy and A. Atala, "3d bioprinting of tissues and organs," *Nature biotechnology*, vol. 32, no. 8, p. 773, 2014.

[28] A. Nadernezhad, N. Khani, G. A. Skvortsov, B. Toprakhisar, E. Bakirci, Y. Menceloglu, S. Unal, and B. Koc, "Multifunctional 3d printing of heterogeneous hydrogel structures," *Scientific reports*, vol. 6, p. 33178, 2016.

[29] A. C. Goodfriend, T. R. Welch, K. T. Nguyen, J. Wang, R. F. Johnson, A. Nugent, and J. M. Forbess, "Poly (gadodiamide fumaric acid): A bioresorbable, radiopaque, and mri-visible polymer for biomedical applications," *ACS Biomaterials Science & Engineering*, vol. 1, no. 8, pp. 677–684, 2015.

[30] M. . A. E. W. J. U. o. T. S. M. C. a. D. D. o. P. C. Ravi, Prashanth; The University of Texas at Arlington, M. Thoracic Surgery Shiakolas, Panos; University of Texas at Arlington, C. Aerospace Engineering Welch, Tre; UT Southwestern Medical Center of Dallas, and T. Surgery, "3d printing of poly (glycerol se-

bacate fumarate) gadodiamide-poly (ethylene glycol) diacrylate structures and characterization of mechanical properties for soft tissue applications," *Journal of Biomedical Materials Research: Part B - Applied Biomaterials*, 2018.

[31] S. S. Daniels, "Tracheomalcia," *Medscape*, 2014.

[32] D. Snijders and A. Barbato, "An update on diagnosis of tracheomalacia in children," *European Journal of Pediatric Surgery*, vol. 25, no. 04, pp. 333–335, 2015.

[33] R. Boogaard, S. H. Huijsmans, M. W. Pijnenburg, H. A. Tiddens, J. C. de Jongste, and P. J. Merkus, "Tracheomalacia and bronchomalacia in children: incidence and patient characteristics," *Chest*, vol. 128, no. 5, pp. 3391–3397, 2005.

[34] R. J. Burden, F. Shann, W. Butt, and M. Ditchfield, "Tracheobronchial malacia and stenosis in children in intensive care: bronchograms help to predict oucome," *Thorax*, vol. 54, no. 6, pp. 511–517, 1999.

[35] S. K. Greenholz, F. M. Karrer, and J. R. Lilly, "Contemporary surgery of tracheomalacia," *Journal of pediatric surgery*, vol. 21, no. 6, pp. 511–514, 1986.

[36] "Advanced treatments for tracheomalacia in children," 2017.

[37] L. Freitag, K. Eicker, T. J. Donovan, and D. Dimov, "Mechanical properties of airway stents." *Journal of Bronchology & Interventional Pulmonology*, vol. 2, no. 4, pp. 270–278, 1995.

[38] K. V. Wong and A. Hernandez, "A review of additive manufacturing," *ISRN Mechanical Engineering*, vol. 2012, 2012.

[39] V. Mironov, V. Kasyanov, and R. R. Markwald, "Organ printing: from bioprinter to organ biofabrication line," *Current opinion in biotechnology*, vol. 22, no. 5, pp. 667–673, 2011.

[40] K. Jakab, C. Norotte, F. Marga, K. Murphy, G. Vunjak-Novakovic, and G. Forgacs, "Tissue engineering by self-assembly and bio-printing of living cells," *Biofabrication*, vol. 2, no. 2, p. 022001, 2010.

[41] B. Mosadegh, G. Xiong, S. Dunham, and J. K. Min, "Current progress in 3d printing for cardiovascular tissue engineering," *Biomedical Materials*, vol. 10, no. 3, p. 034002, 2015.

[42] P. Ravi, P. S. Shiakolas, T. Welch, T. Saini, K. Guleserian, and A. K. Batra, "On the capabilities of a multi-modality 3d bioprinter for customized biomedical devices," in *ASME 2015 International Mechanical Engineering Congress and Exposition*. American Society of Mechanical Engineers, 2015, pp. V02AT02A008–V02AT02A008.

[43] P. Ravi, P. S. Shiakolas, and A. D. Thorat, "Analyzing the effects of temperature, nozzle-bed distance, and their interactions on the width of fused deposition modeled struts using statistical techniques toward precision scaffold fabrication," *Journal of Manufacturing Science and Engineering*, vol. 139, no. 7, p. 071007, 2017.

[44] S. K. Panda, S. Padhee, S. Anoop Kumar, and S. Mahapatra, "Optimization of fused deposition modelling (fdm) process parameters using bacterial foraging technique," *Intelligent information management*, vol. 1, no. 02, p. 89, 2009.

[45] D. Chimene, K. K. Lennox, R. R. Kaunas, and A. K. Gaharwar, "Advanced bioinks for 3d printing: a materials science perspective," *Annals of biomedical engineering*, vol. 44, no. 6, pp. 2090–2102, 2016.

[46] P. Mohan Pandey, N. Venkata Reddy, and S. G. Dhande, "Slicing procedures in layered manufacturing: a review," *Rapid prototyping journal*, vol. 9, no. 5, pp. 274–288, 2003.

[47] P. Ravi *et al.*, "Towards the fabrication of bioresorbable constructs with customized properties using additive manufacturing," Ph.D. dissertation, 2017.

[48] P. Ravi, P. S. Shiakolas, J. C. Oberg, S. Faizee, and A. K. Batra, "On the development of a modular 3d bioprinter for research in biomedical device fabri-

cation," in *ASME 2015 International Mechanical Engineering Congress and Exposition*. American Society of Mechanical Engineers, 2015, pp. V02AT02A059–V02AT02A059.

[49] P. Sitthi-Amorn, J. E. Ramos, Y. Wangy, J. Kwan, J. Lan, W. Wang, and W. Matusik, "Multifab: a machine vision assisted platform for multi-material 3d printing," *ACM Transactions on Graphics (TOG)*, vol. 34, no. 4, p. 129, 2015.

[50] R. Anitha, S. Arunachalam, and P. Radhakrishnan, "Critical parameters influencing the quality of prototypes in fused deposition modelling," *Journal of Materials Processing Technology*, vol. 118, no. 1-3, pp. 385–388, 2001.

[51] T. Nancharaiah, "Optimization of process parameters in fdm process using design of experiments," *Int J Emerg Technol*, vol. 2, no. 1, pp. 100–102, 2011.

[52] T. Ang, F. Sultana, D. Hutmacher, Y. S. Wong, J. Fuh, X. Mo, H. T. Loh, E. Burdet, and S.-H. Teoh, "Fabrication of 3d chitosan–hydroxyapatite scaffolds using a robotic dispensing system," *Materials science and engineering: C*, vol. 20, no. 1-2, pp. 35–42, 2002.

[53] S. Khalil, J. Nam, and W. Sun, "Multi-nozzle deposition for construction of 3d biopolymer tissue scaffolds," *Rapid Prototyping Journal*, vol. 11, no. 1, pp. 9–17, 2005.

[54] Y. Yan, Z. Xiong, Y. Hu, S. Wang, R. Zhang, and C. Zhang, "Layered manufacturing of tissue engineering scaffolds via multi-nozzle deposition," *Materials Letters*, vol. 57, no. 18, pp. 2623–2628, 2003.

[55] R. Chang, J. Nam, and W. Sun, "Effects of dispensing pressure and nozzle diameter on cell survival from solid freeform fabrication–based direct cell writing," *Tissue Engineering Part A*, vol. 14, no. 1, pp. 41–48, 2008.

[56] K. Dhal, "On the development and integration of pneumatic extrusion module and a methodology to identify process parameters for additive manufacturing

using machine learning," 2018.